August 22, 2003

FCC ID# NI3-AT53V114

Applicant: Senao International Co. Ltd.
Correspondence Reference Number: 25608
731 Confirmation Number: EA246449

SAR Report originally submitted: July 17, 2003

1. *Please submit mix procedures for 5 GHz liquid.*

Response:

As given in Table 2, we have tried three different fluids (fluids 2, 3, 4) for SAR determination in the 5 GHz band and found all of them to be capable of giving the expected/calculated peak 1-g SAR for the FCC-recommended body-simulant fluid [1] within ±1.5%. Because of the desirable transparency of fluid 5 consisting of sugar/water/HEC, we used this fluid for 1-g SAR determination of the EUT. For this composition, HEC and sugar were mixed thoroughly and water added gradually thereafter. The mixture was stirred as more and more water was added to dissolve HEC/sugar combination into water.

2. *Please submit printout/output/screen-dump from dielectric test system icluding several frequencies within band.*

Response:

At the outset, it must be mentioned that no tissue-simulant fluids have been suggested in any of the existing standards or draft standards for 1- or 10-g SAR determination for personal wireless devices for frequencies above 3 GHz [1-4]. Because of this limitation, some of the standards are only written for frequencies up to 3 GHz [e.g. refs. 2, 3]. During the last several months, we have looked at over 40 liquid mixtures of the following broad categories to decide on a fluid that would give the peak 1-g SAR for 802.11a antennas operating at frequencies 5.15 to 5.35 and 5.745 to 5.845 GHz that are comparable to those obtained for the FCC-recommended dielectric properties [1]. The categories of fluids studied for determination of dielectric properties (ε', ε'') using Hewlett Packard Model 85070B Dielectric Probe and the latest software 85070d provided by the company are:

a. Deionized water.
b. Deionized water and HEC mixtures (with HEC being 1-4%).
c. Deionized water, polyethylene powder (PEP) and HEC mixtures.
d. Mannitol, deionized water, HEC mixtures.
e. Sugar, deionized water, HEC mixtures.

The screen-dumps for some of the representative fluids studied are given in Figs. 1-5, respectively. For each of the cases, the conductivity σ for the fluid may be obtained by

multiplying ε'' by $\omega\varepsilon_o$ where $\omega = 2\pi f$ and ε_o is the permittivity of free space, 8.854×10^{-12} F/m. The measured ε', σ thus determined for frequencies of 5.25 and 5.8 GHz typical of 802.11a band are given in Table 1. Looking at Table 1, it is clear that the dielectric properties for pure deionized water are undesirable (the dielectric constant is too high even though the conductivities σ are no more than 10% larger than the desired values); the deionized water/PEP/HEC mixture and mannitol/water/HEC combinations are quite acceptable with dielectric constants within 1-3% and conductivities within 6-12% of the desired values. However, these two fluids have an undesirable feature that they are not transparent. The sugar/water/HEC mixture, on the other hand, is transparent. While giving the dielectric constants ε' that are within 1-3% of the desired values, the conductivity of this otherwise desirable fluid is about 27-30% higher than the desired values.

It was decided to determine SAR distributions and peak 1-g SARs for the three somewhat desirable fluids marked 3, 4, and 5 using an open-ended waveguide (WR187) as an irradiator that has been proposed for SAR system validation [5, attached as Appendix A]. Given in Table 2 are the peak 1-g SARs determined for fluids 3, 4, and 5 (of Table 1). Also given for comparison is the FDTD-calculated values both at 5.25 and 5.8 GHz using an FDTD-grid size of 0.5 mm for the dielectric properties recommended by FCC ($\varepsilon' = 48.9$, $\sigma = 5.36$ S/m for 5.25 GHz; $\varepsilon' = 48.2$, $\sigma = 6.00$ S/m at 5.8 GHz). It is most interesting to note that in spite of up to 30% higher conductivity for the sugar/water/HEC fluid 5 (of Table 1), the peak 1-g SAR is within ± 1.5% of that for the FCC-recommended dielectric properties [1] both at 5.25 and 5.86 Hz. This result was most surprising and led us to a detailed study of the effect of dielectric properties on the peak 1- and 10-g SAR for the 802.11a frequencies described as a part of the paper that has been accepted for publication in *IEEE Transactions on Electromagnetic Compatibility* [6, attached as Appendix B]. In this study, we have taken conductivities that are up to 150% of the values recommended by FCC [1] at 5.25 and 5.8 GHz to show that the peak 1-g SARs vary by no more than ± 2% for typical near-field sources such as a waveguide and a microstrip antenna of dimensions typical of 802.11a antennas (see Tables 1, 2 of Appendix B). As explained in [6], this is due to higher surface SAR but shallower depth of penetration of EM fields for the higher conductivity media resulting in nearly identical SARs for cubical volumes associated with 1- or 10-g of tissue, respectively. This point is illustrated in Figs. 6 and 7 for 5.25 and 5.8 GHz, respectively.

3. *SAR report refers to deionized water and methanol dielectric tests – please describe test procedures and include measured values, at least for deionized water compared to theoretical.*

Response:

The measured variation of ε' and ε'' for deionized water is given in Fig. 1. The values $\varepsilon' = 72.97$, $\sigma = 5.54$ S/m at 5.25 GHz and $\varepsilon' = 71.82$, $\sigma = 6.61$ S/m at 5.8 GHz given in Table 1 (fluid1) are in good agreement with theoretical values for deionized water.

4. *What is the distance from bottom of card slot to flat phantom for lapheld position (Configuration 1)?*

Response:

The distance from bottom of the card slot to flat phantom for lapheld position (Configuration 1) is 13.7 mm.

5. *Please submit close-up edge view photo of card in laptop slot.*

Response:

A close-up edge view photograph of card in laptop slot is attached here as Fig. 8.

6. *EMC and SAR reports show identical output powers. SAR report refers to these as average powers, EMC as peak. Please describe procedures used to ensure card was transmitting at max power for SAR tests, including average power test results as appropriate.*

Response:

This is a typo. The caption of Table 1 on p.12 of the SAR test report submitted on July 17,2003 should read ' Peak conducted RF power outputs' rather than 'Average conducted RF power outputs'.
The procedure for conducted output power measurements used the channel power function of the spectrum analyzer Model FSEK 30. The procedure and the results obtained for the various channels are given in Appendix C.

REFERENCES

[1] FCC "Evaluating Compliance with FCC Guidelines for Human Exposure to Radiofrequency Electromagnetic Fields," Supplement C (Edition 01-01) to OET Bulletin 65, June 2001.

[2] European Standard EN50361, "Basic Standard for the Measurement of Specific Absorption Rate Related to Human Exposure to Electromagnetic Fields from Mobile Phones (300 MHz-3 GHz)," CENELEC, Central Secretariat: rue de Stassart 35, B-1050, Brussels.

[3] IEEE Standard 1528-2003, "Recommended Practice for Determining the Peak Spatial-Average Specific Absorption Rate (SAR) in the Human Body Due to Wireless Communications Devices: Experimental Techniques," Institute of Electrical and Electronics Engineers, New York, NY 10016.

[4] Draft IEC PT62209 Part 2, "Procedure to Measure the Specific Absorption Rate (SAR) for Two-Way Radios, Palmtop Terminals, Laptop Terminals, Desktop Terminals, and Body-Mounted Devices Including Accessories and Multiple Transmitters (30 MHz to 6 GHz)," Draft version 0.6.

[5] Q. Li, O. P. Gandhi, and G. Kang, "An Open-Ended Waveguide System for SAR System Validation and/or Probe Calibration for Frequencies above 3 GHz," submitted for publication to *IEEE Transactions on Microwave Theory and Techniques*, June 2003 (attached here as Appendix A).

[6] G. Kang and O. P. Gandhi, "Effect of Dielectric Properties on the Peak 1- and 10-g SAR for 802.11 a/b/g Frequencies 2.45 and 5.15 to 5.85 GHz," accepted for publication in *IEEE Transactions on Electromagnetic Compatibility* (attached here as Appendix B).

Table 1. The measured dielectric constants and conductivities σ for some fluids for frequencies 5.25 and 5.8 GHz.

Fluid	5.25 GHz		5.8 GHz	
	ε′	σ S/m	ε′	σ S/m
1. Deionized water	72.97	5.54	71.82	6.61
2. Deionized water (96%), HEC (4%)	68.89	5.81	67.78	6.90
3. Deionized water (82%), polyethylene powder (16%), HEC (2%)	49.31	4.77	47.99	5.64
4. Mannitol (31.5%), deionized water (67.5%), HEC (1%)	47.59	5.80	47.30	6.74
5. Sugar (31%), deionized water (68.0%), HEC (1%)	48.79	6.82	46.86	7.83

Table 2. Comparison of the measured and calculated peak 1-g SAR at 5.25 and 5.8 GHz.

	5.25 GHz			5.8 GHz		
	ε′	σ S/m	1-g SAR W/kg	ε′	σ S/m	1-g SAR W/kg
FCC body [1]; calculated	48.9	5.36	3.57	48.2	6.00	3.95
Fluid 3 of Table 1, water/PEP/HEC; measured	49.3	4.77	3.55	48.0	5.64	3.91
Fluid 4 of Table 1, Mannitol/water/HEC; measured	47.6	5.80	3.59	47.3	6.74	3.93
Fluid 5 of Table 1, sugar/water/HEC; measured	48.8	6.82	3.62	46.9	7.83	3.94

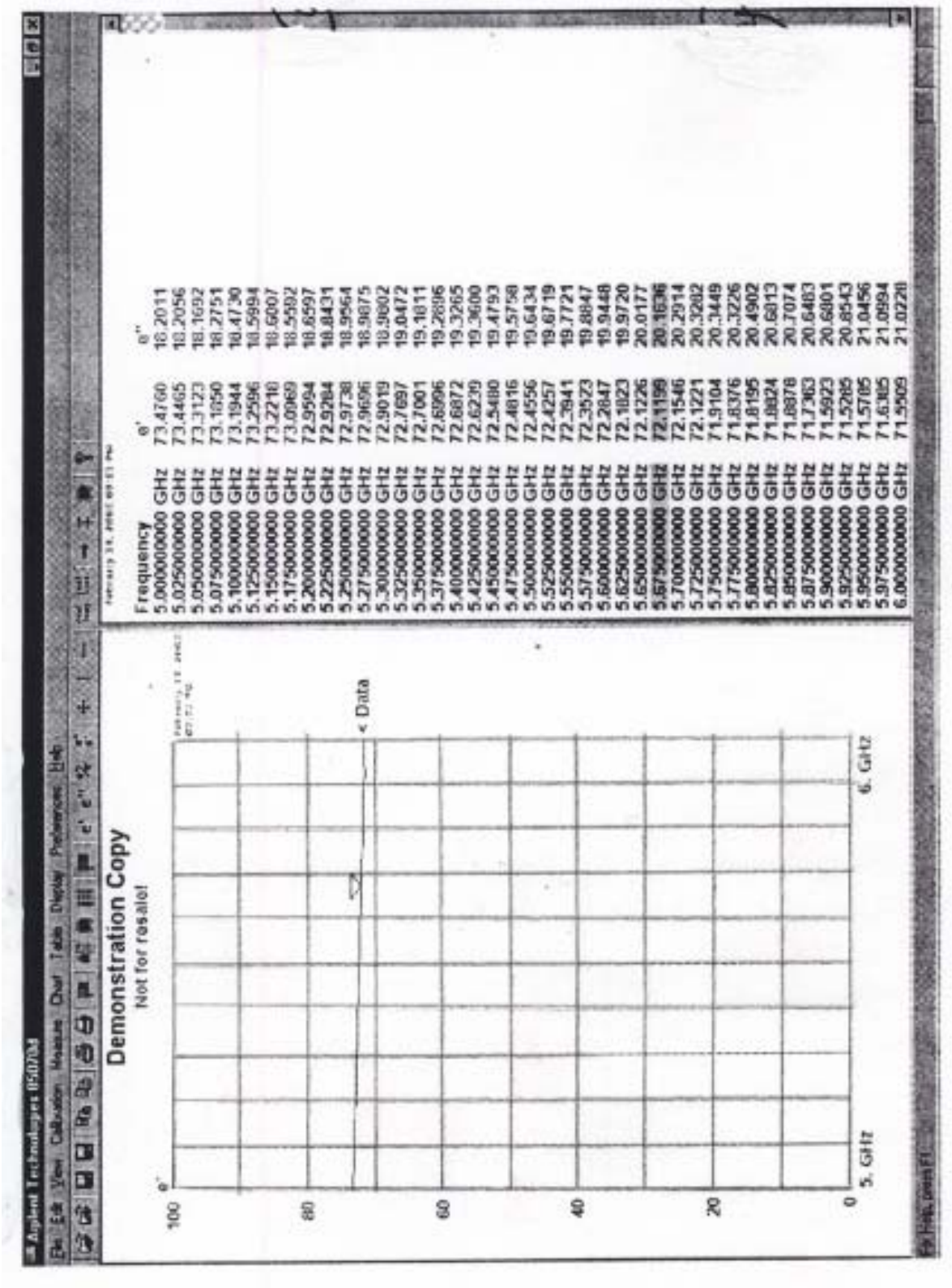

Fig. 1. The output of the measured ε', ε'' for deionized water for the frequency band 5 to 6 GHz.

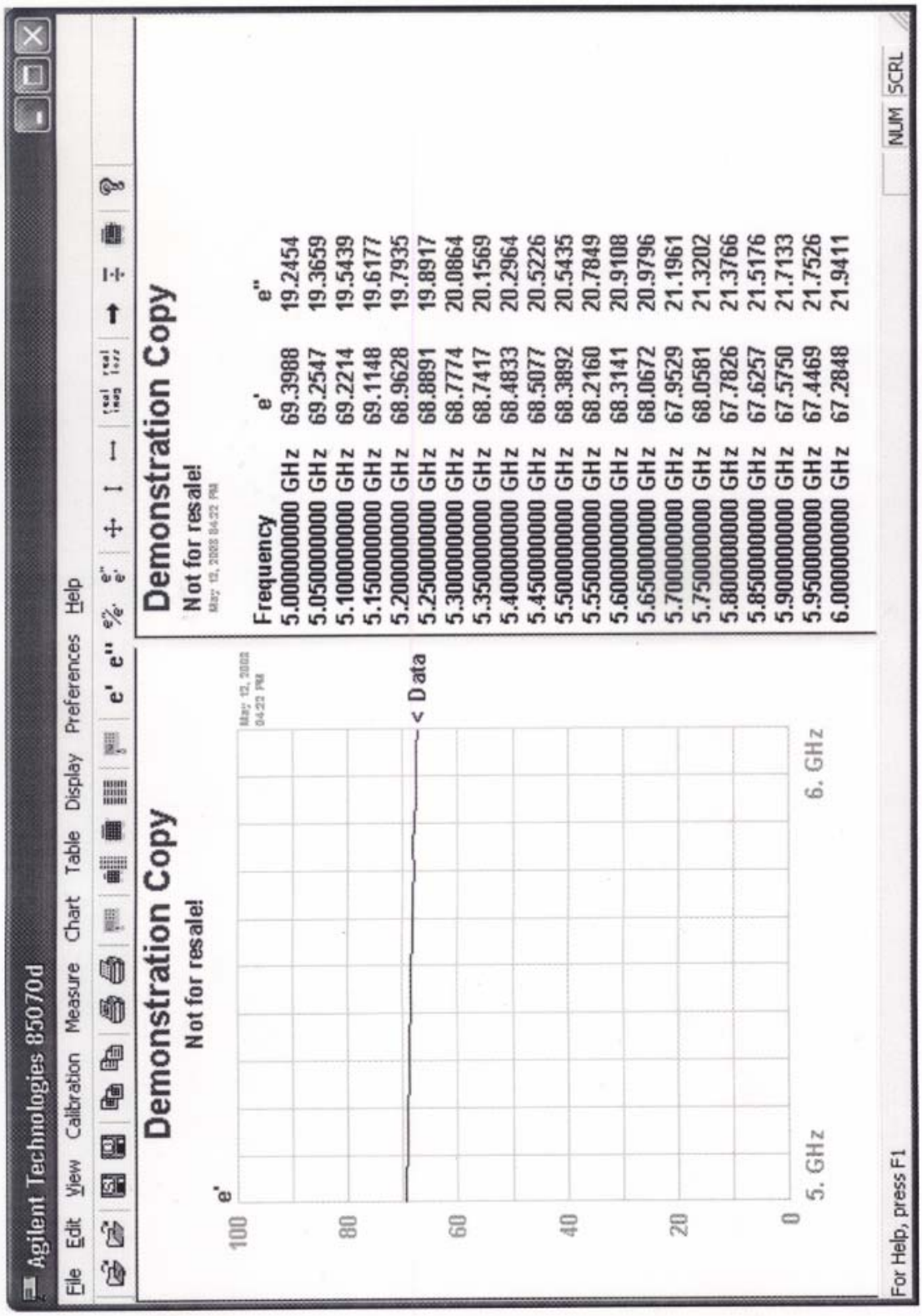

Fig. 2. The measured ε', ε'' for a composition of 96% deionized water and 4% HEC for the frequency band 5 to 6 GHz.

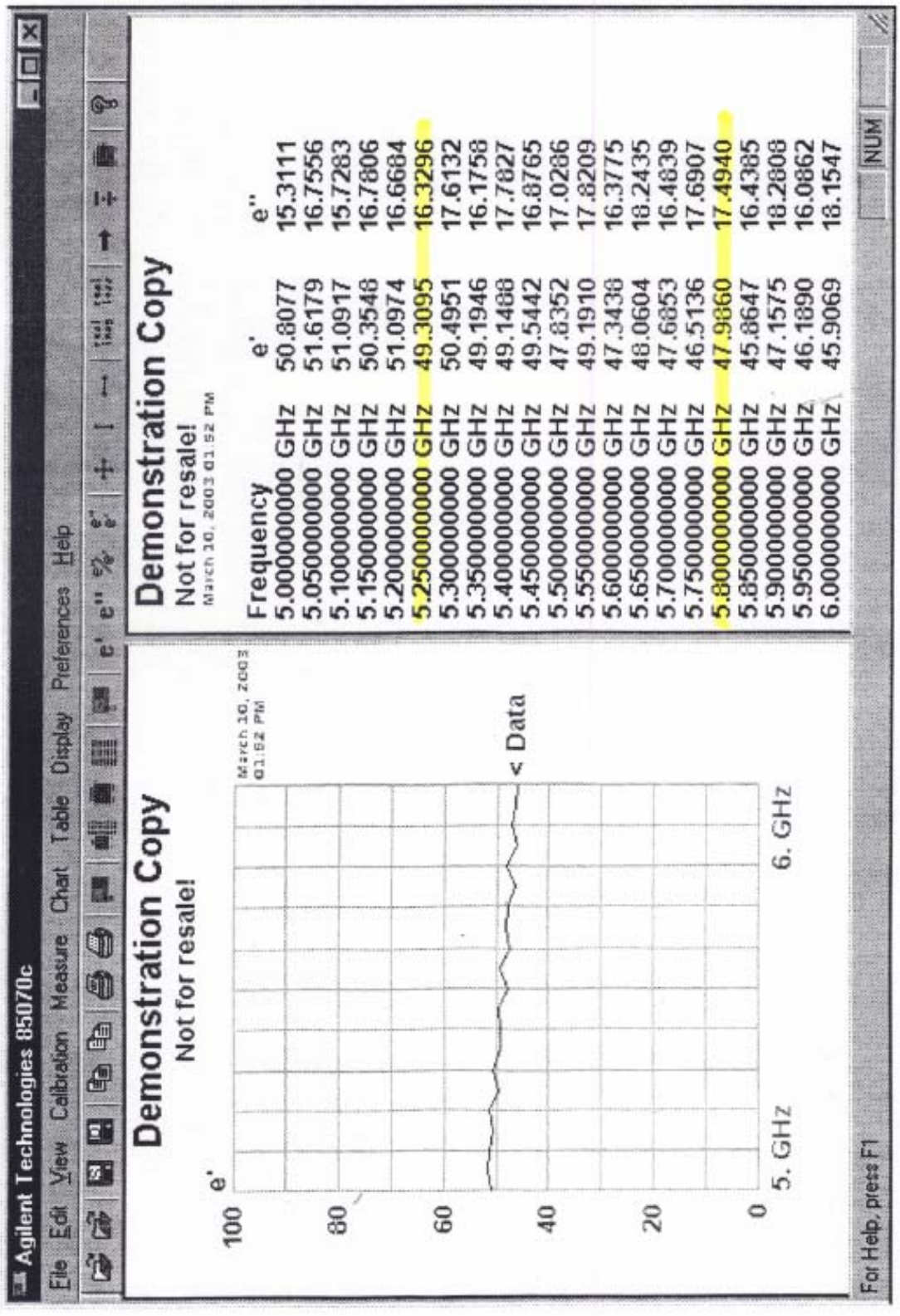

Fig. 3. The measured ε', ε'' for a composition of 82% deionized water, 16% polyethylene powder and 2% HEC for the frequency band 5 to 6 GHz.

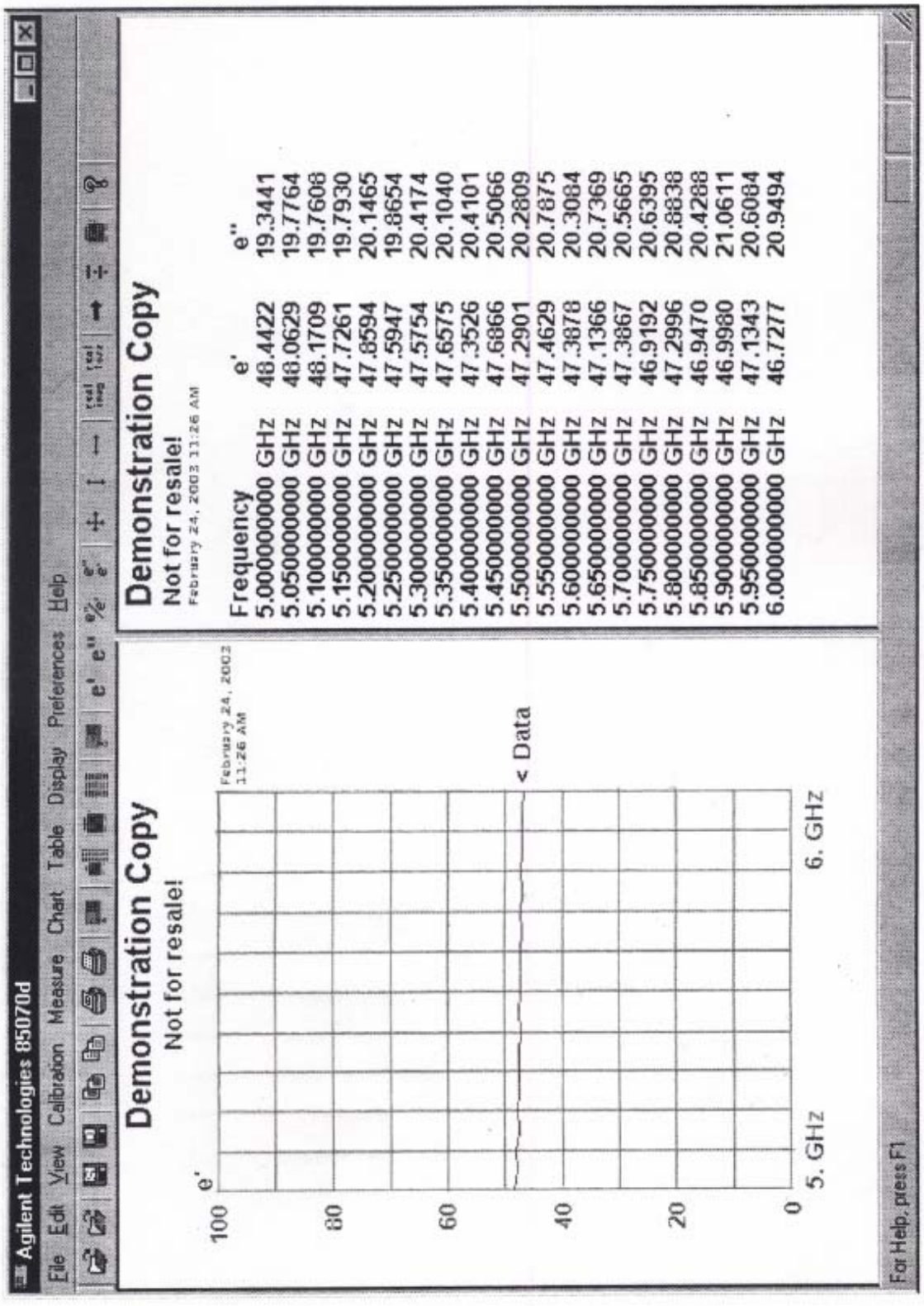

Fig. 4. The measured ε', ε'' for a composition of 31.5% mannitol, 67.5% deionized water, and 1% HEC for the frequency band 5 to 6 GHz.

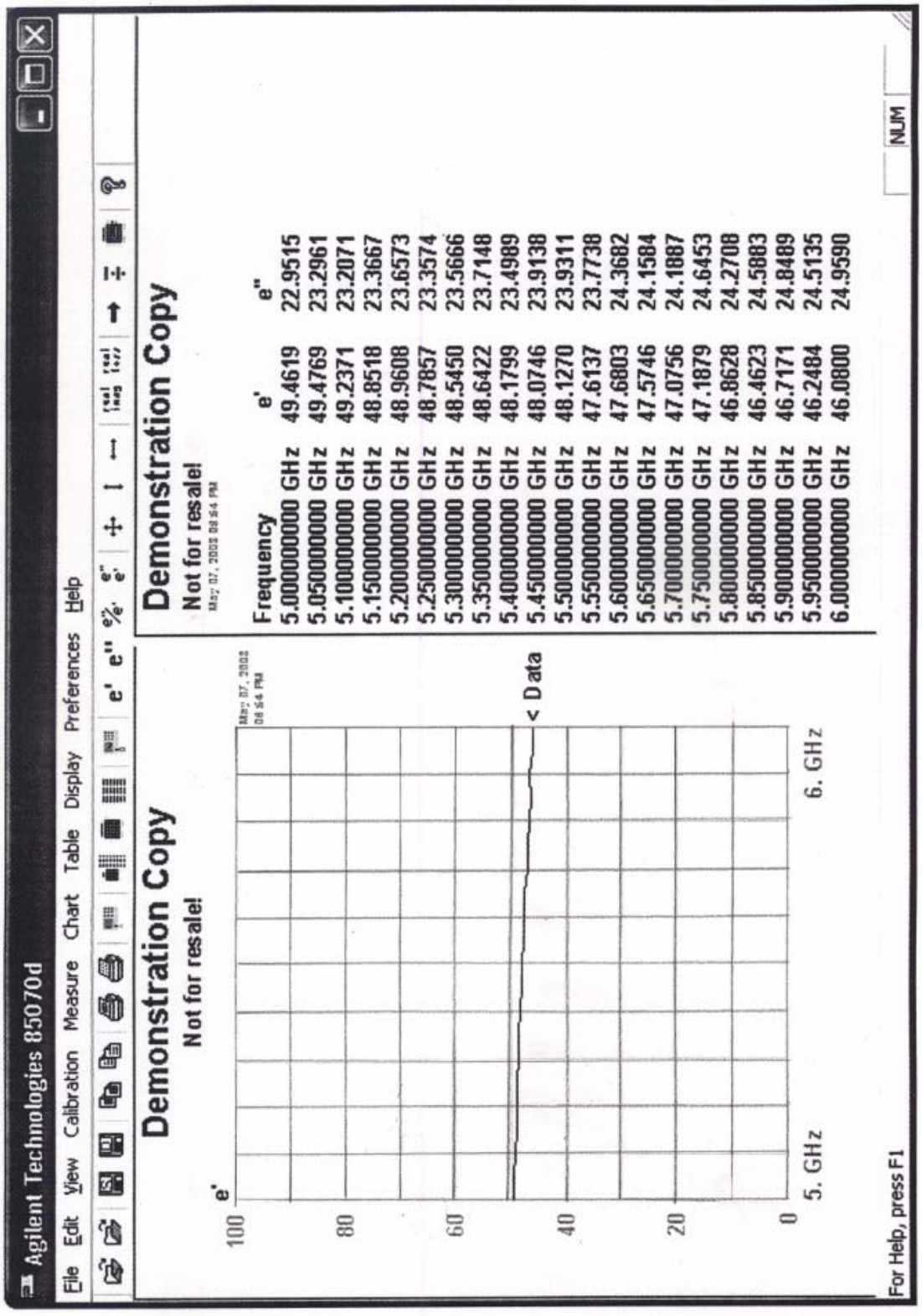

Fig. 5. The measured ε', ε'' for a composition of 31% sugar, 68% deionized water, and 1% HEC for the frequency band 5 to 6 GHz.

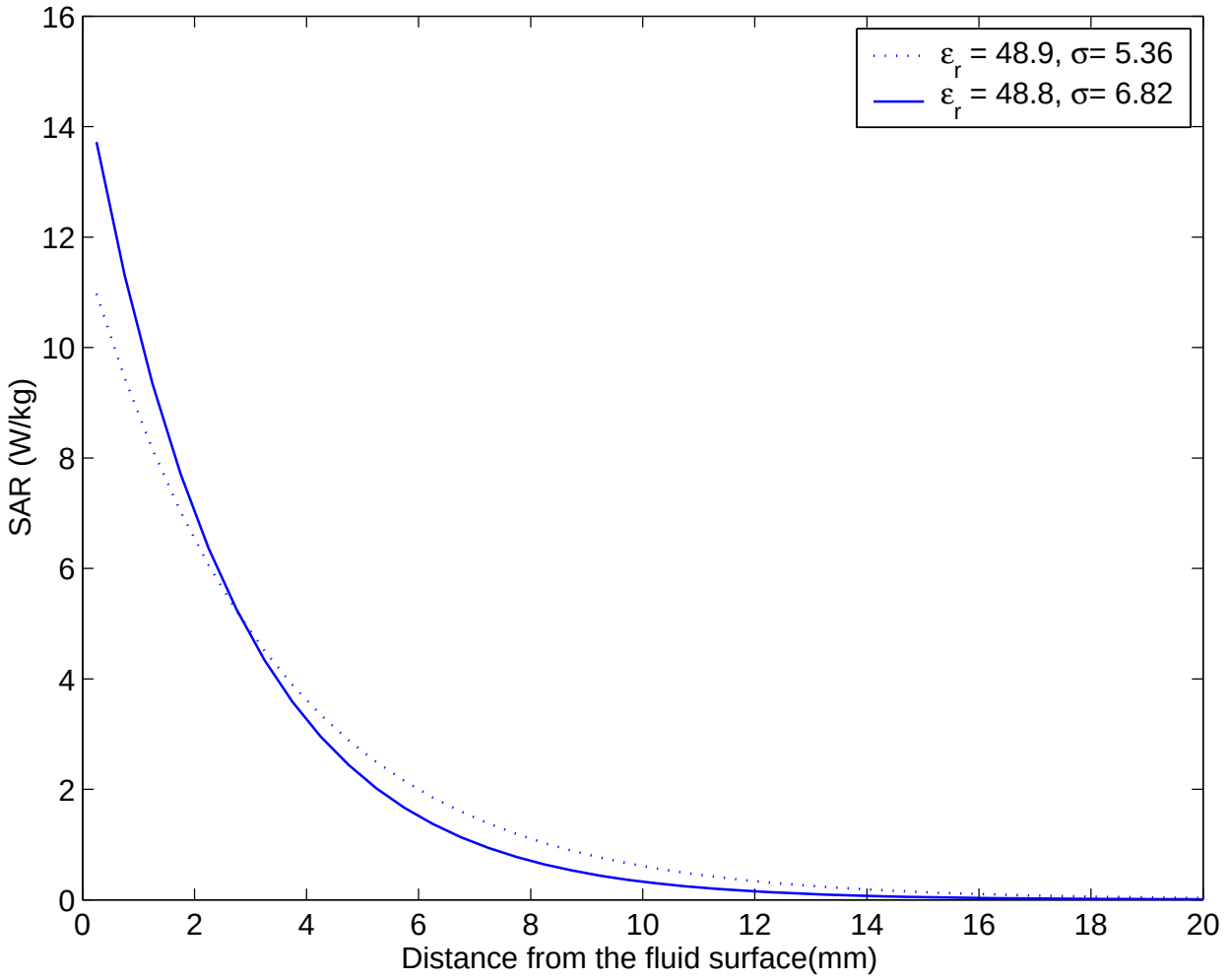

Fig. 6. Comparison of the FDTD-calculated variations of the SAR with depth for the FCC-recommended dielectric properties ($\varepsilon' = 48.9$, $\sigma = 5.36$ S/m) and the sugar/water/HEC fluid 5 ($\varepsilon' = 48.8$, $\sigma = 6.82$ S/m) at **5.25 GHz**. Assumed for calculations is the WR187 rectangular waveguide radiator placed 10 mm below the bottom surface of the tissue-simulant fluid in a flat phantom of base thickness 2 mm with ($\varepsilon_r = 2.56$). Radiated power = 100 mW.

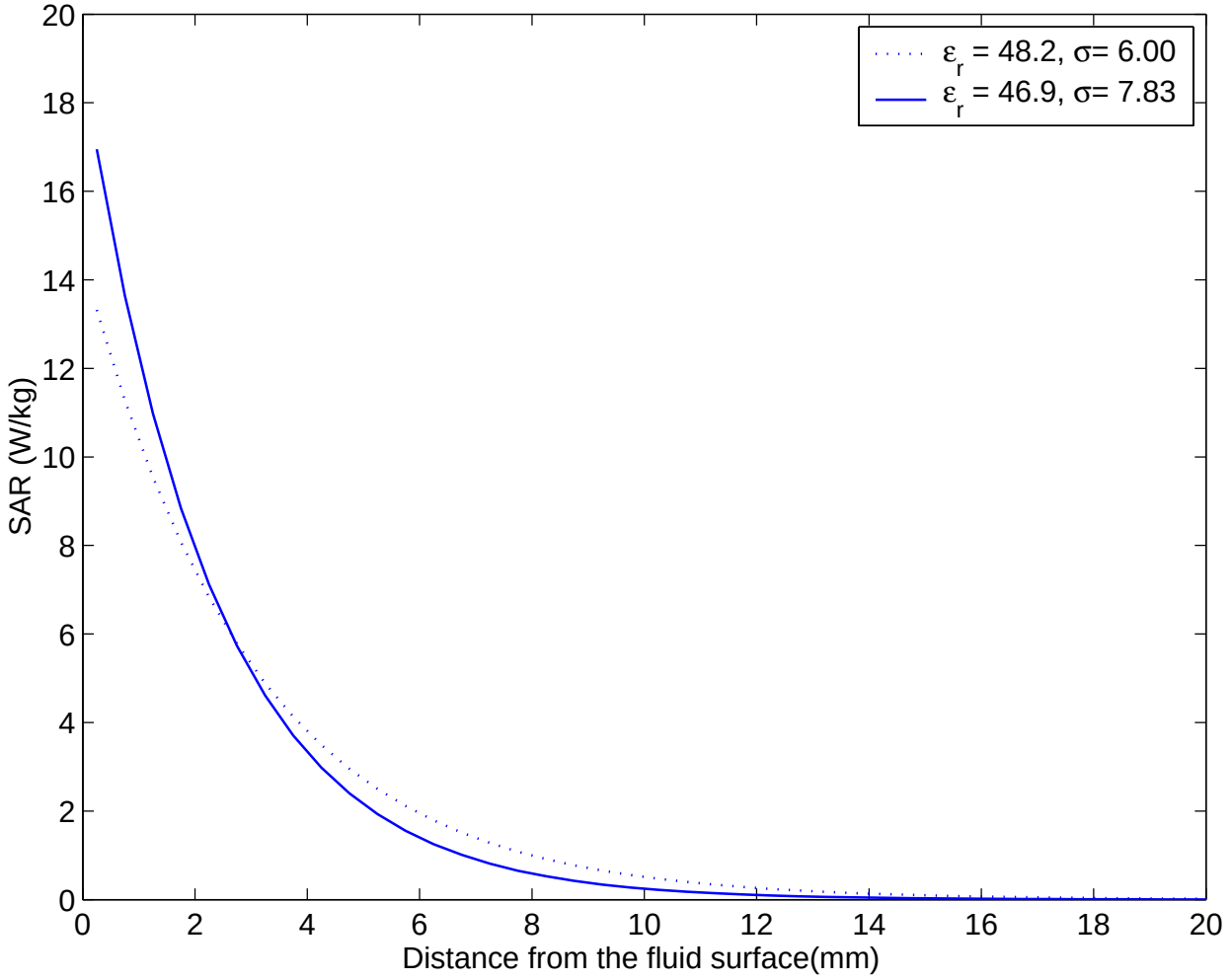

Fig. 7. Comparison of the FDTD-calculated variations of the SAR with depth for the FCC-recommended dielectric properties ($\varepsilon' = 48.2$, $\sigma = 6.00$ S/m) and the sugar/water/HEC fluid 5 ($\varepsilon' = 46.9$, $\sigma = 7.83$ S/m) at **5.8 GHz**. Assumed for calculations is the WR187 rectangular waveguide radiator placed 10 mm below the bottom surface of the tissue-simulant fluid in a flat phantom of base thickness 2 mm with ($\varepsilon_r = 2.56$). Radiated power = 100 mW.

Fig. 8. Close-up edge view of the Senao Wireless Cardbus Adapter inserted into IBM Model 2659 Notebook Computer.

APPENDIX A

AN OPEN-ENDED WAVEGUIDE SYSTEM FOR SAR SYSTEM VALIDATION AND/OR PROBE CALIBRATION FOR FREQUENCIES ABOVE 3 GHz

Qingxiang Li, Student Member, IEEE
Om P. Gandhi, Life Fellow, IEEE, and
Gang Kang, Senior Member, IEEE
Department of Electrical and Computer Engineering
University of Utah
Salt Lake City, Utah 84112, U.S.A.

Abstract

Compliance with safety guidelines prescribed in terms of maximum electromagnetic power absorption (specific absorption rate or SAR) for any 1- or 10-g of tissue is required for all newly-introduced personal wireless devices such as Wi-Fi PCs. The prescribed SAR measuring system is a planar phantom with a relatively thin base of thickness 2.0 mm filled with a lossy fluid to simulate dielectric properties of the tissues. A well-characterized, broadband irradiator is required for SAR system validation and/or submerged E-field probe calibration for the new 802.11a frequencies in the 5-6 GHz band. We describe an open-ended waveguide system that may be used for this purpose. Using a fourth-order polynomial least-square fit to the experimental data gives SAR variations close to the bottom surface of the phantom that are in excellent agreement with those obtained using the FDTD numerical method. The experimentally-determined peak 1-g SARs are within 1 to 2 percent of those obtained using the FDTD both at 5.25 and 5.8 GHz.

Index Terms – Broadband, electromagnetic exposure system, probe calibration, safety assessment, comparison with numerical calculations

Submitted to *IEEE Transactions on Microwave Theory and Techniques*, June 10, 2003

AN OPEN-ENDED WAVEGUIDE SYSTEM FOR SAR SYSTEM VALIDATION AND/OR PROBE CALIBRATION FOR FREQUENCIES ABOVE 3 GHz

Qingxiang Li, Student Member, IEEE
Om P. Gandhi, Life Fellow, IEEE, and
Gang Kang, Senior Member, IEEE

I. Introduction

Compliance with the safety guidelines such as those proposed by IEEE [1] ICNIRP [2], etc. is required by regulatory agencies in the United States and elsewhere for all newly-introduced personal wireless devices such as Wi-Fi PCs, cellular telephones, etc. These safety guidelines are set in terms of maximum 1- or 10-g mass-normalized rates of electromagnetic energy deposition (specific absorption rates or SARs) for any 1- or 10-g of tissue. The two most commonly-used SAR limits today are those of IEEE [1] – 1.6 W/kg for any 1 g of tissue, and ICNIRP [2] – 2 W/kg for any 10 g of tissue, excluding extremities such as hands, wrists, feet, and ankles where higher SARs up to 4 W/kg for any 10 g of tissue are permitted in both of these standards. Experimental and numerical techniques using planar or head-shaped phantoms have been proposed for determining compliance with the SAR limits [3-5]. For frequencies above 800 MHz, the size of a rectangular waveguide is quite manageable and use of an appropriate waveguide filled with a tissue-simulant medium is recommended for calibration of an E-field probe in FCC Supplement C, Edition 01-01 to OET Bulletin 65 [6]. Even though no recommendation is made on choice of an irradiation system for frequencies above 3 GHz, balanced half-wave dipoles have been suggested for system validation for frequencies less than or equal to 3 GHz [6]. It is very difficult to develop half-wave dipole antennas for use in the 5.1 to 5.8 GHz band both because of fairly small dimensions and the resulting dimensional tolerances, and relatively narrow bandwidths of the required baluns – balanced to unbalanced transformers (typically less than 10-12% for VSWR < 2.0 and less than 5-6% for VSWR < 1.5). On the other hand, rectangular waveguides are broadband with simultaneous bandwidths larger than 1-2 GHz and are fairly easy to use for frequencies in excess of 3 GHz. We have, therefore, developed an open-ended waveguide system for SAR system validation and/or probe calibration in the frequency band 5 to 6 GHz. This is a band that is presently being used for 802.11a antennas of Wi-Fi PCs.

II. The Waveguide Irradiation System

For the 5-6 GHz band, we have used a WR187 rectangular waveguide of internal dimensions 4.75 × 2.21 cm. The operating (TE_{10} mode) band of this waveguide is from 3.95 to 5.85 GHz. This is considerably larger than the required overall bandwidth of 675 MHz for the IEEE 802.11a frequency bands of 5.15-5.35 and 5.745 to 5.825 GHz. The waveguide irradiation system used for SAR system validation is shown in Fig. 1. As recommended in [6], the open-ended waveguide irradiator is placed at a distance of 8 mm below the base of planar phantom with inside dimensions of 30.5 × 41.9 cm and a base thickness of 2.0 ± 0.2 mm. This results in the open end of the waveguide at a distance of 10 mm below the lossy tissue-simulant fluid in the phantom. The microwave circuit arrangement used for the waveguide irradiation system is

shown in Fig. 2. As shown in Fig. 2, the WR187 waveguide is fed with microwave power from a Hewlett Packard Model 83620A Synthesized Sweeper (10 MHz-20 GHz). When placed at a distance of 8 mm below the base of the planar phantom, the reflection coefficient is about 10-20%. Even this relatively small amount of reflection has been greatly reduced to less than 0.5% by using a movable slide-screw waveguide tuner (Narda Model 22CI). The planar phantom is filled to a depth of 15 cm with a fluid to simulate dielectric properties recommended for the body phantom in [6]. The dielectric constants ε_r and conductivities σ at the experimental frequencies of 5.25 and 5.8 GHz are similar to those recommended in the SAR Compliance Standards used in the U.S. and in Europe [3, 4]. For our experiments and calculations $\varepsilon_r = 48.8$, $\sigma = 6.82$ S/m at 5.25 GHz; and $\varepsilon_r = 46.9$, $\sigma = 7.83$ S/m at 5.8 GHz.

Fig. 1. Photograph of the rectangular waveguide radiator used for system validation. Also seen is the Narda Model 22CI movable slide screw tuner used to match the input power at 5.25 or 5.8 GHz to the planar tissue-simulant phantom.

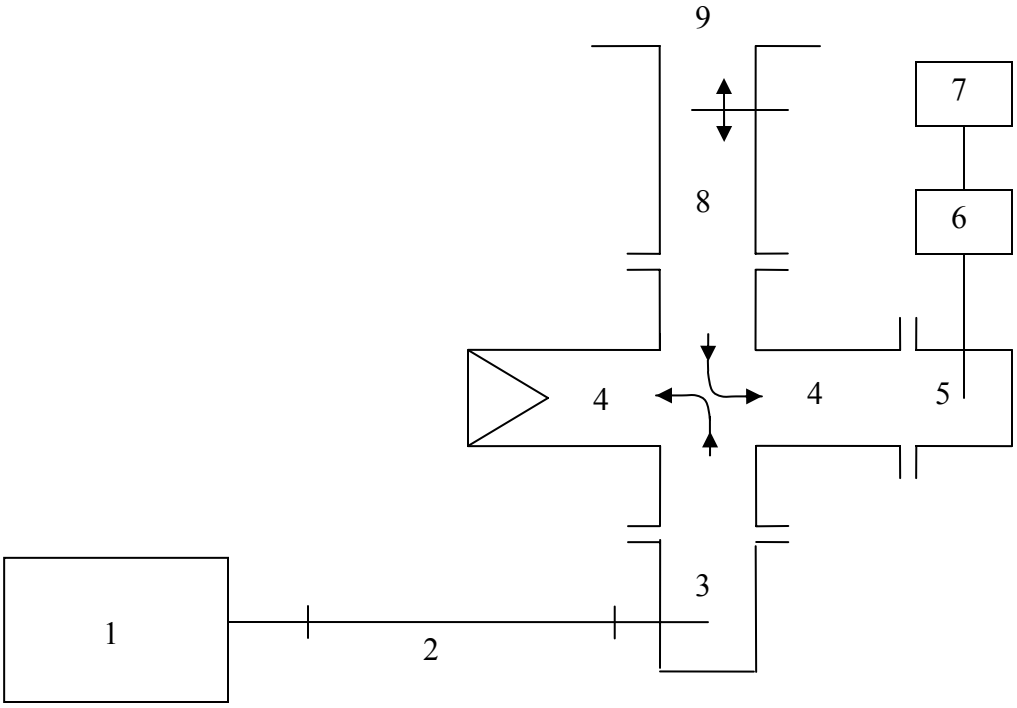

1. Hewlett Packard (HP) Model 83620A Synthesized Sweeper (10 MHz-20 GHz).
2. Coaxial line.
3. Coaxial to waveguide adapter.
4. 20 dB crossguide coupler (may be reversed to measure incident power).
5. HP Model G281A coaxial to waveguide adapter
6. HP Model 8482A power sensor.
7. HP Model 436A power meter.
8. Narda Microline® Slide Screw Tuner Model 22CI.
9. Radiating open end of the waveguide.

Fig. 2. The microwave circuit arrangement used for SAR system validation.

III. Calculation of the SAR Distributions

We have used the well-established finite-difference time-domain (FDTD) numerical electromagnetic method to calculate the electric fields and SAR distributions for the planar phantom of base thickness 2.0 mm of dielectric constant $\varepsilon_r = 2.56$ and dielectric properties of the tissue-simulant lossy fluid as given in Section II. The FDTD method described in several texts [7, 8] has been successfully used by various researchers [9-12] and, therefore, would not be described here. For the FDTD calculations, we have used a cell size $\delta = 0.5$ mm in order to meet the requirement $\delta \leq \lambda_\varepsilon / 10$ in the lossy fluid. The calculated variations of the SAR distribution at the experimental frequencies of 5.25 and 5.80 GHz are given in Figs. 3 a-c and 4

a-c, respectively. Also shown in the same figures are the experimental values of the SARs (shown by circles). From Figs. 3 and 4, it is obvious that the penetration of electromagnetic fields in the 5.1 to 5.8 GHz band is extremely shallow. The calculated depths of penetration corresponding to $1/e^2$-reduction of SAR (13.5% of the SAR at the surface) are only 6.85 and 5.985 mm at 5.25 and 5.8 GHz, respectively. Both of these depths of penetration are very similar to those obtained for plane-wave irradiation at these frequencies (7.15 mm for 5.25 GHz and 6.25 mm for 5.8 GHz).

IV. Experimental Setup and Measurements

A. *Experimental Setup*

As recommended in FCC Bulletin 65 [14], a planar phantom of fairly thin base thickness 2.0 mm of relatively low dielectric constant ($\varepsilon_r = 2.56$ in our case) is used for the determination of SAR distributions of wireless PCs and for the SAR system validation. The lateral dimensions of the planar phantom (in our case 30.5 × 41.9 cm) are large enough to ignore scattering from the edges of the rectangular box or the tissue-simulant lossy fluid used to fill this box to a depth of 10-15 cm (several times the depth of penetration of fields in the fluid so as to present a nearly infinitely deep medium to neglect reflections). A photograph of the phantom model together with a computer-controlled 3-D stepper motor system (Arrick Robotics MD-2A) is shown in Fig. 5.

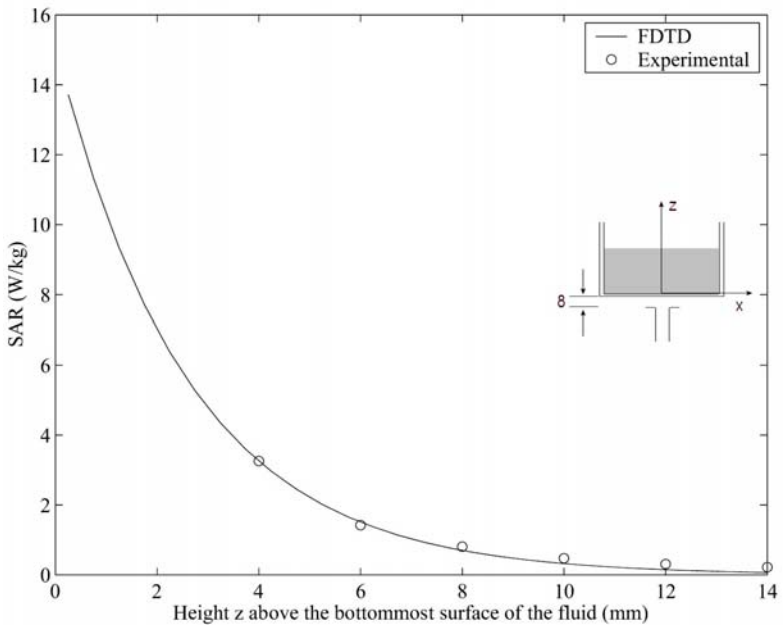

a. Variation of SAR along the z-axis.

Fig. 3. Comparison of the measured and calculated SAR variations for a planar phantom of base thickness 2.0 mm and internal dimensions 30.5 × 41.9 × 20 cm for a WR 187 open-ended waveguide radiator placed 10 mm below the bottommost surface of the lossy tissue-simulant phantom. Frequency = 5.25 GHz.

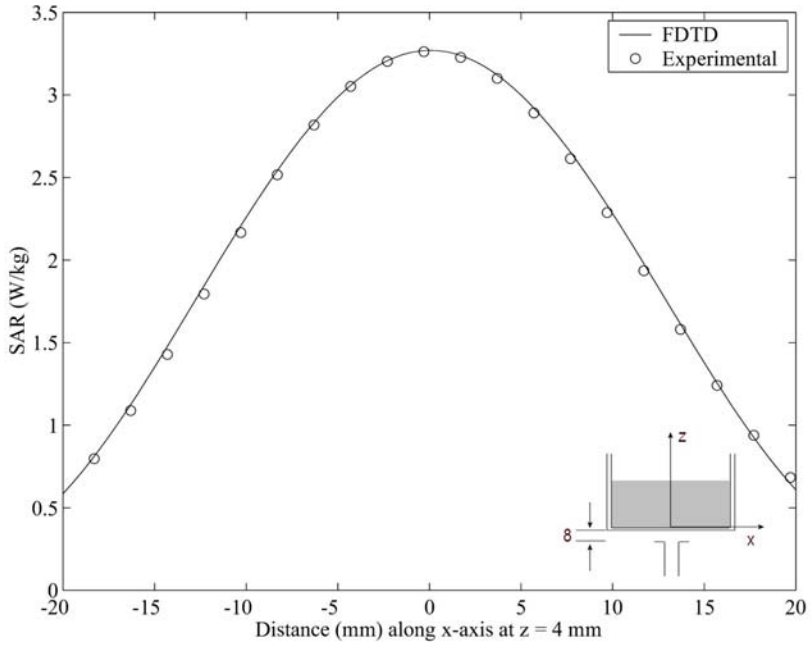

b. Variation of SAR along the x-axis parallel to the broader dimension of the waveguide at height z = 4 mm.

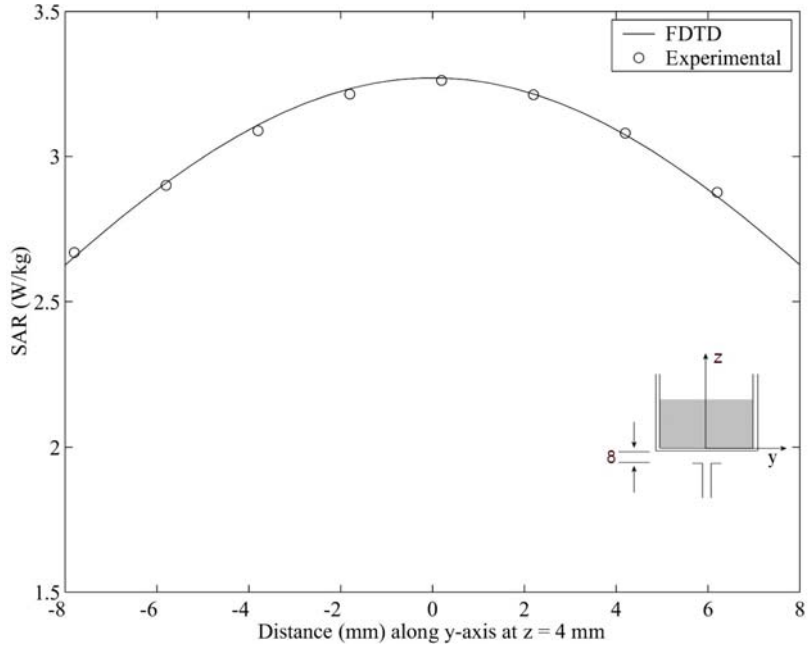

c. Variation of SAR along the y-axis parallel to the narrower dimension of the waveguide at height z = 4 mm.

Fig. 3. Comparison of the measured and calculated SAR variations for a planar phantom of base thickness 2.0 mm and internal dimensions 30.5 × 41.9 × 20 cm for a WR 187 open-ended waveguide radiator placed 10 mm below the bottommost surface of the lossy tissue-simulant phantom. Frequency = 5.25 GHz.

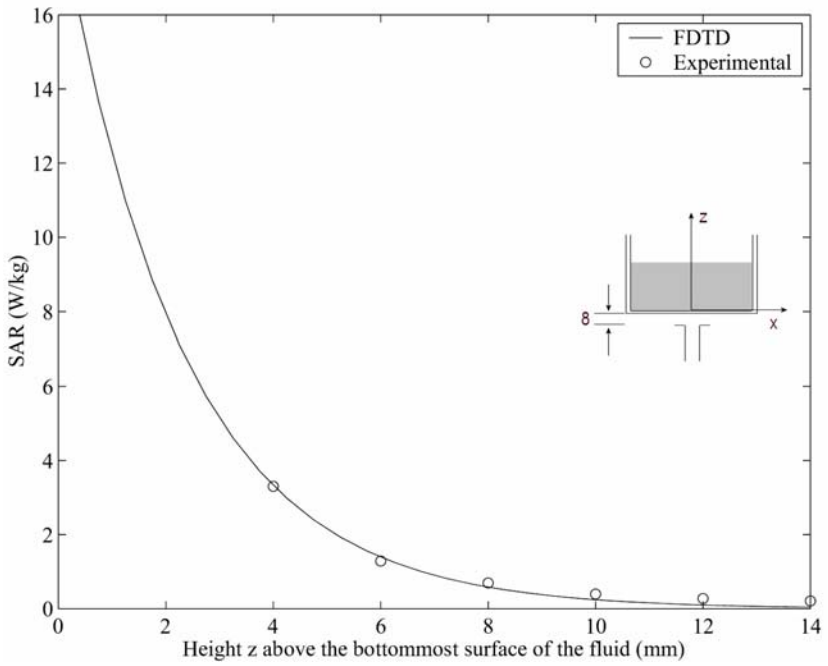

a. Variation of SAR along the z-axis.

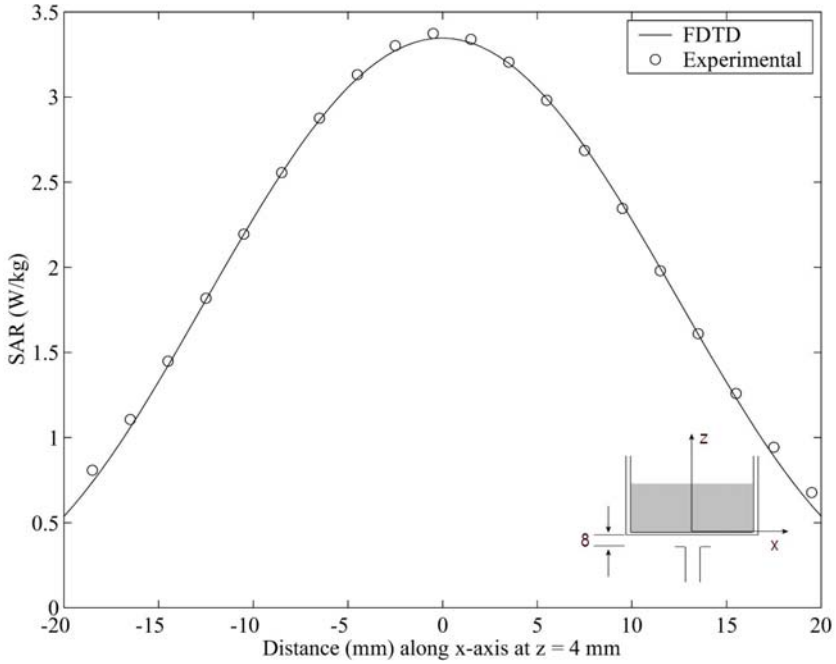

b. Variation of SAR along the x-axis parallel to the broader dimension of the waveguide at height z = 4 mm.

Fig. 4. Comparison of the measured and calculated SAR variations for a planar phantom of base thickness 2.0 mm and internal dimensions 30.5 × 41.9 × 20 cm for a WR 187 open-ended waveguide radiator placed 10 mm below the bottommost surface of the lossy tissue-simulant phantom. Frequency = 5.8 GHz.

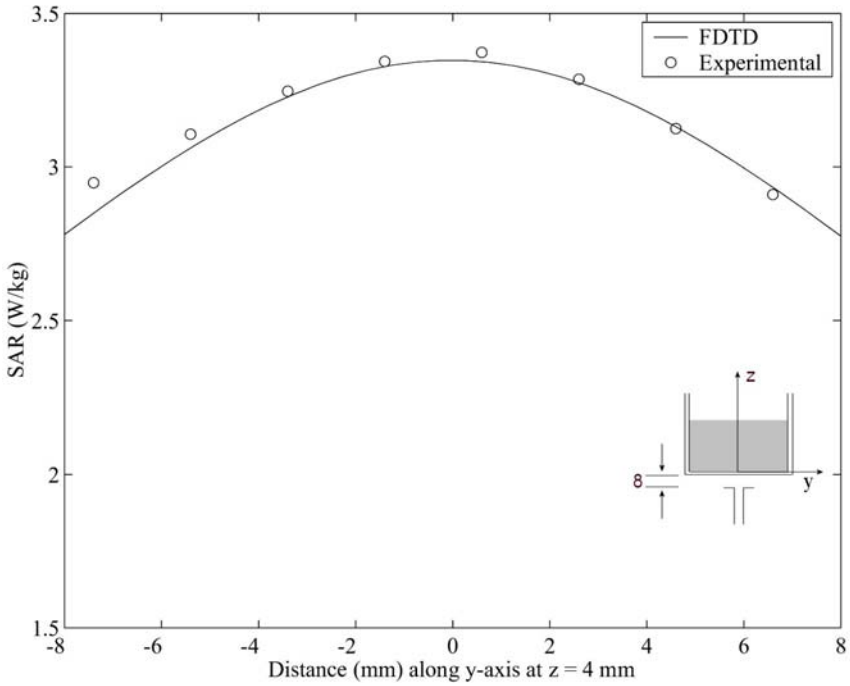

c. Variation of SAR along the y-axis parallel to the narrower dimension of the waveguide at height z = 4 mm.

Fig. 4. Comparison of the measured and calculated SAR variations for a planar phantom of base thickness 2.0 mm and internal dimensions 30.5 × 41.9 × 20 cm for a WR 187 open-ended waveguide radiator placed 10 mm below the bottommost surface of the lossy tissue-simulant phantom. Frequency = 5.8 GHz.

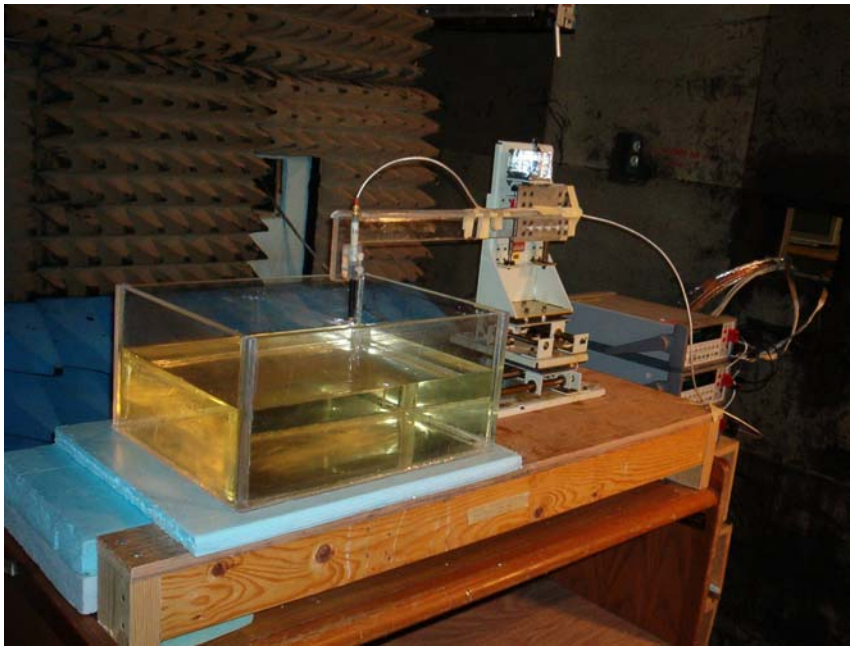

Fig. 5. Photograph of the planar model with the 3-D stepper motor system used for measurement of SAR variation for comparison with FDTD calculations.

A triaxial Narda Model 8021 E-field probe is used to determine the internal electric fields. The positioning repeatability of the stepper motor system moving the E-field probe is within ± 0.1 mm. Outputs from the three channels of the E-field probe are dc voltages, the sum of which is proportional to the square of the internal electric fields ($|E_i|^2$) from which the SAR can be obtained from the equation: SAR = $\sigma(|E_i|^2)/\rho$, where σ and ρ are the conductivity and mass density of the tissue-simulant material, respectively [13]. The dc voltages for the three channels of the E-field probe are read by three HP 34401A multimeters and sent to the computer via an HPIB interface. The setup is carefully grounded and shielded to reduce the noise due to the electromagnetic interference (EMI).

B. ***E-Field Probe***

The nonperturbing implantable E-field probe used in the setup was originally developed by Bassen et al. [14] and is manufactured by L3/Narda Microwave Corporation, Hauppauge, NY as Model 8021 E-field probe. In the probe, three orthogonal miniature dipoles each of length approximately 2.5 mm are placed on a triangular-beam substrate. Each dipole is loaded with a small Schottky diode and connected to the external circuitry by high resistance ($2\ \mathrm{M}\Omega \pm 40\%$) leads to reduce secondary pickups. The entire structure is then encapsulated with a low dielectric constant insulating material. The probe thus constructed has a very small diameter (4 mm), which results in a relatively small perturbation of the internal electric field. The probe is rated for frequencies up to 3 GHz for tissue-simulant media, but is presently used for system validation at frequencies in the 5 to 6 GHz range. Consequently, the probe had to be checked for square-law performance, and isotropy for use at these higher frequencies.

1. **Test for Square-Law Region:** It is necessary to operate the E-field probe in the square-law region for each of the diodes so that the sum of the dc voltage outputs from the three dipoles is proportional to the square of the internal electric field ($|E_i|^2$). Fortunately, the personal wireless devices such as the PCs induce SARs that are generally less than 5-6 W/kg even for closest locations to the body. For SAR measurements, it is, therefore, necessary that the E-field probe be checked for square-law behavior for SARs up to such values that are likely to be encountered. Such a test may be conducted using a canonical lossy body such as a rectangular box used here. By varying the radiated power of the waveguide, the output of the probe should increase linearly with the applied power for each of the test locations.

   Shown in Fig. 6a and b are the results of the tests performed to check the square-law behavior of the E-field probe used in our setup at 5.25 and 5.8 GHz, respectively. Used as the radiator is the WR 187 waveguide placed at a distance of 8 mm below the base of the planar phantom (10 mm below the bottom surface of the tissue-simulant fluid as recommended in [6]).

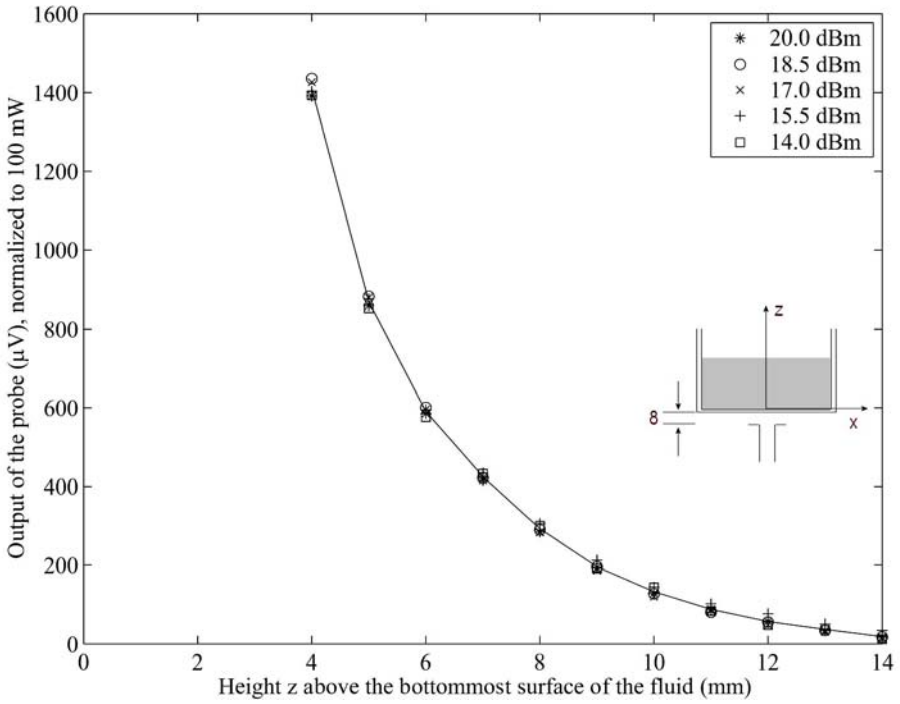

a. Test for square-law behavior at 5.25 GHz.

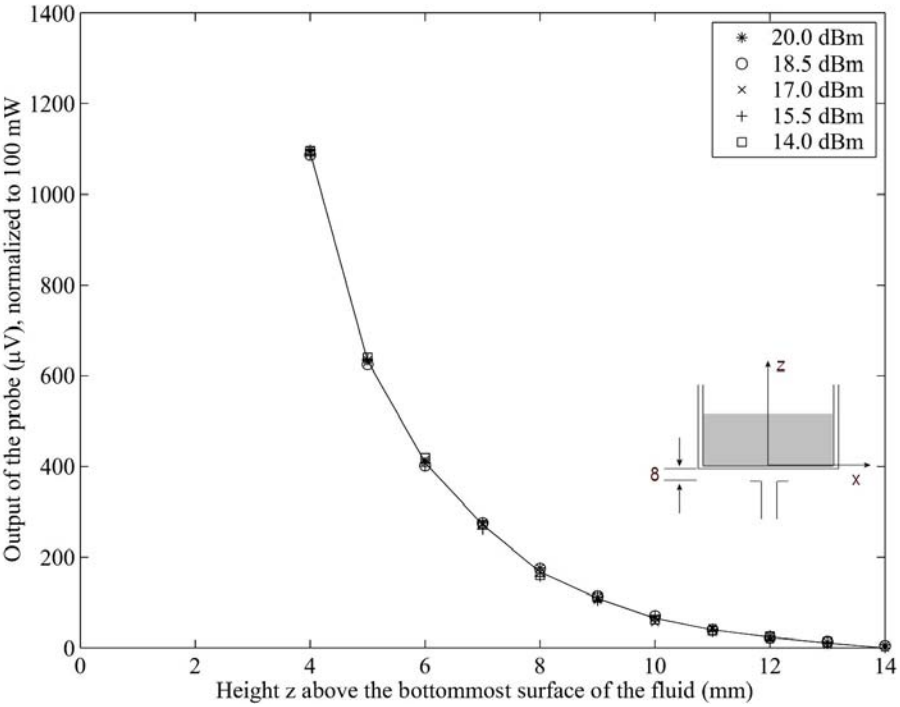

b. Test for square-law behavior at 5.8 GHz.

Fig. 6. Variation of the output voltage (proportional to $|E_i|^2$) for different radiated powers normalized to 100 mW (20 dBm).

Since the dc voltage outputs of the probe are fairly similar when normalized to a radiated power of 100 mW, the square-law behavior is demonstrated and an output voltage that is proportional to $|E_i|^2$ is obtained within ± 2.2% both at 5.25 and 5.8 GHz.

2. **Test for Isotropy of the Probe:** Another important characteristic of the probe that affects the measurement accuracy is its isotropy. Since the orientation of the induced electric field is generally unknown, the E-field probe should be relatively isotropic in its response to the orientation of the E-field. Shown in Fig. 7a and b are the test results of the E-field probe used in our setup at 5.25 and 5.8 GHz, respectively. The E-field probe was rotated around its axis from 0-180° in incremental steps of 15°. Because of the alternating nature of the fields, angles of θ and 180° + θ are identical, hence 0-165° rotation of the E-field probe was considered to be adequate to cover the entire 360° rotation of the probe. As seen in Fig. 7a and b, an isotropy of less than ± 0.18 dB (± 4.3%) was observed for this E-field probe both at 5.25 and 5.8 GHz.

3. **Calibration of the E-Field Probe:** Since the voltage output of the E-field probe is proportional to the square of the internal electric field ($|E_i|^2$), the SAR is, therefore, proportional to the voltage output of the E-field probe by a proportionality constant C. The constant C is defined as the calibration factor and is frequency and material dependent. It is measured to calibrate the probe at the various frequencies of interest using the appropriate tissue-simulating materials for the respective frequencies.

   Canonical geometries such as waveguides, rectangular slabs, and layered or homogeneous spheres have, in the past, been used for the calibration of the implantable E-field probe [15-17] albeit at lower frequencies. Since the FDTD method has been carefully validated to solve electromagnetic problems for a variety of near-field exposure geometries [18], we were able to calibrate the Narda E-field probe by comparing the measured variations of the probe voltage (proportional to $|E_i|^2$) against the FDTD-calculated variations of the SARs for the planar phantom of base thickness 2.0 mm ($\varepsilon_r = 2.56$) and internal dimensions 30.5 × 41.9 × 20 cm irradiated by the WR 187 waveguide placed below this phantom as previously described in Section. II. Shown in Figs. 6a, b and 7a, b are the comparisons between the experimentally measured and FDTD-calculated variations of the SAR distributions in the tissue-simulant fluid. Since there are excellent agreements between the calculated SARs and the measured variations of the voltage outputs of the E-field probe, it is possible to calculate the calibration factors at the respective frequencies by fitting the measured data to the FDTD-calculated results by means of the least mean-square error (LMSE) method. For the Narda Model 8021 E-field probe used in our setup, the calibration factor is determined to be 2.98 (mW/kg)/μV ± 5% both at 5.25 and 5.8 GHz, respectively.

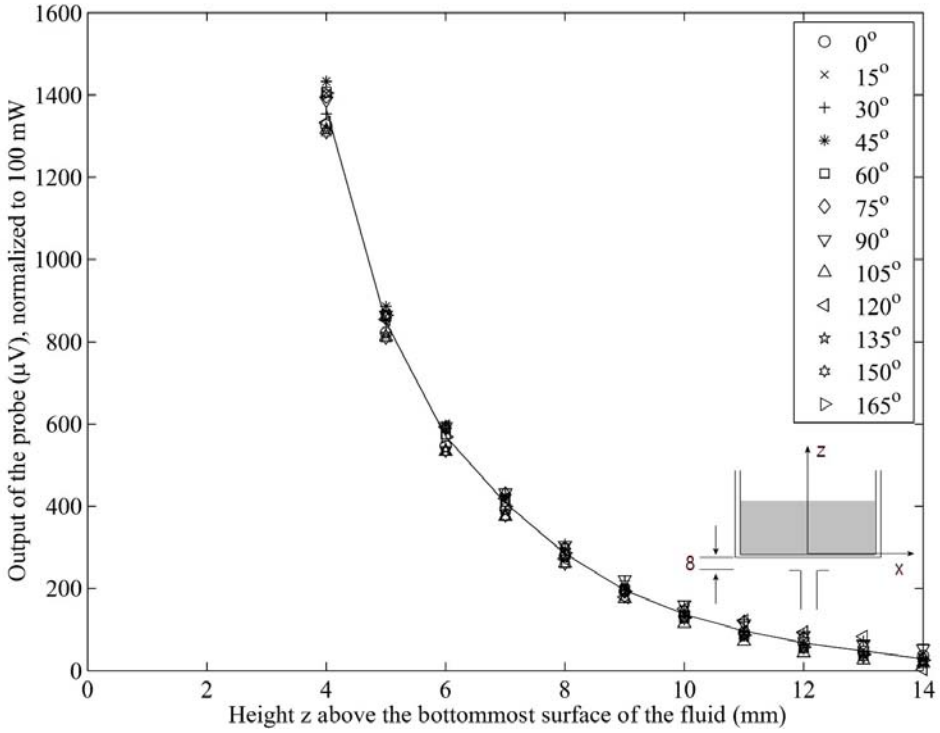

a. 5.25 GHz.

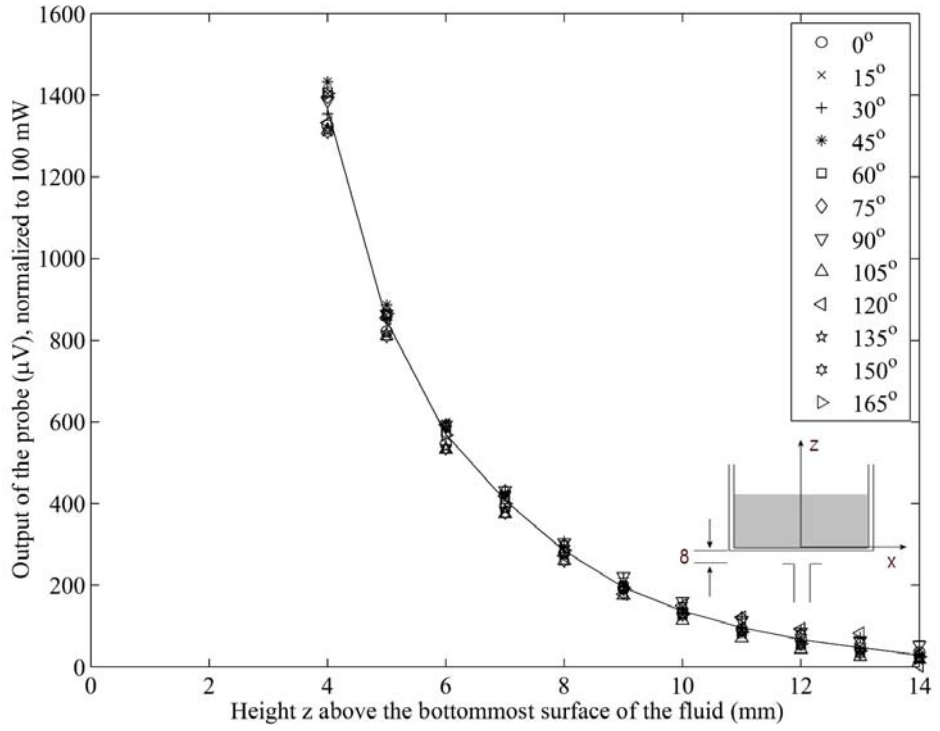

b. 5.8 GHz.

Fig. 7. Test for isotropy.

V. Need for Extrapolation

Because of the physical separation of the three orthogonal pickup dipoles from the tip of the E-field probe, the SAR measurements cannot be taken any closer than about 3 mm from the bottom surface of the phantom fluid. As given in Figs. 8 and 9, we have measured the SARs with 2 mm resolution at heights of 4, 6, 8, 10, 12 and 14 mm above the bottom surface of the phantom fluid. We have tried second-, third-, fourth-, and fifth-order polynomial least-square fits to extrapolate the measured data to obtain SARs closer to the bottom of the lossy fluid. As seen in Figs. 8 and 9, the second- and third-order polynomials underestimate the SARs while the fifth-order polynomial overestimates the SAR distribution. An excellent least-square fit to the numerically-calculated SAR variations is obtained by using a fourth-order polynomial to extrapolate the measured data both at 5.25 and 5.8 GHz.

After identifying the region of the highest SAR, the SAR distributions were measured with a finer resolution of 2 mm in order to obtain the peak 1 cm^3 or 1-g SAR. Here too, the SAR measurements were performed for the xy planes at heights z of 4, 6, 8, 10, 12, and 14 mm from the bottom surface of the body-simulant fluid. The SARs thus measured were extrapolated using a fourth-order least-square fit to the measured data to obtain values at 1, 3, 5, 7, and 9 mm height and used to obtain peak 1-g SARs. For a radiated power of 100 mW, the SARs thus obtained with 2 mm resolution for xy planes at heights z of 1, 3, 5, 7, and 9 mm for the peak SAR region of volume 10 ×10 × 10 mm were used to obtain peak 1-g SAR at 5.25 and 5.8 GHz, respectively. The experimentally-determined peak 1-g SARs for 100 mW of radiated power of 3.678 and 3.947 W/kg are extremely close to the FDTD-calculated 1-g SARs for this waveguide irradiator of 3.580 and 3.946 W/kg at 5.25 and 5.80 GHz, respectively.

V. Conclusions

We have developed an open-ended waveguide irradiation system for validation of the SAR measurement system and/or for E-field probe calibration in the 802.11a frequency band 5.15 to 5.825 GHz. A fourth-order polynomial least-square fit to the experimental data gives SAR variations close to the bottom surface of the phantom that are in excellent agreement with those obtained using the FDTD method. The experimentally-determined peak 1-g SARs are within 1 to 2 percent of those obtained using the FDTD numerical calculations.

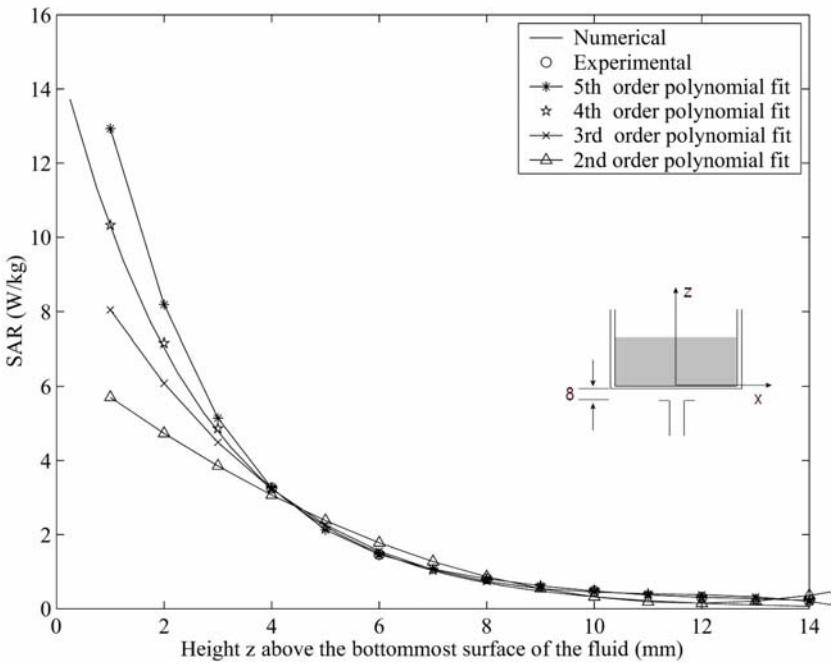

Fig. 8. Comparison of the experimentally measured and FDTD-calculated variation of the SAR with depth in the body-simulant planar phantom at 5.25 GHz. Also shown are the SARs extrapolated from experimental values to heights of 1, 3, 5, 7 and 9 mm above the bottom of the phantom using second-, third-, fourth-, and fifth-order least-square fit polynomials.

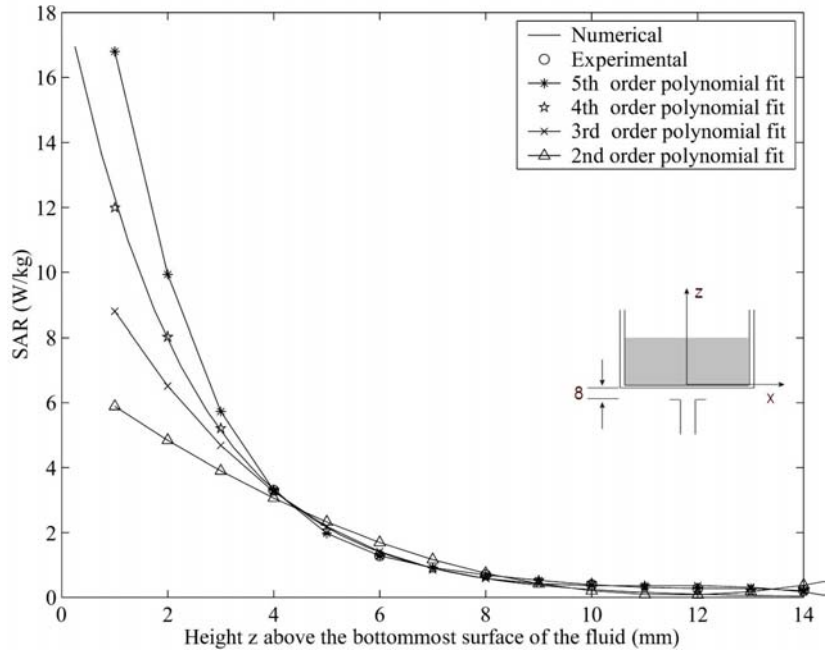

Fig. 9. Comparison of the experimentally measured and FDTD-calculated variation of the SAR with depth in the body-simulant planar phantom at 5.8 GHz. Also shown are the SARs extrapolated from experimental values to heights of 1, 3, 5, 7 and 9 mm above the bottom of the phantom using second-, third-, fourth-, and fifth-order least-square fit polynomials.

REFERENCES

1. IEEE Std. C95.1, "IEEE Standard for Safety Levels with Respect to Human Exposure to Radiofrequency Electromagnetic Fields, 3 kHz to 300 GHz," Institute of Electrical and Electronics Engineers, Piscataway, NJ, 1999.

2. ICNIRP (International Commission on Non-Ionizing Radiation Protection), "Guidelines for limiting exposure to time-varying electric, magnetic, and electromagnetic fields (up to 300 GHz)", *Health Physics*, Vol. 74, pp. 494-522, 1998.

3. IEEE Standards Coordinating Committee 34 Draft Standard, "Recommended Practice for Determining the Peak Spatial-Average Specific Absorption Rate (SAR) in the Human Body Due to Wireless Communications Devices: Experimental Techniques," Institute of Electrical and Electronics Engineers, 2002.

4. CENELEC EN50361, "Basic Standard for Measurement of Specific Absorption Rate Related to Human Exposure to Electromagnetic Fields from Mobile Telephones (300-MHz-3 GHz), CENELEC European Committee for Electrotechnical Standardization, rue de Stassart 35, B-1050, Brussels, Belgium.

5. IEC TC 106/PT62209, "Evaluation of Human Exposure to Radiofrequency Fields from Handheld and Body-Mounted Wireless Communications Devices in the Frequency Range of 30 MHz to 6 GHz: Human Models, Instrumentation Procedures," Draft Standard in preparation, 2003.

6. U.S. Federal Communications Commission (FCC), "Additional Information for Evaluating Compliance of Mobile and Portable Devices with FCC Limits for Human Exposure to Radiofrequency Emissions," Supplement C Edition 01-01 to OET Bulletin 65 Edition 97-01, June 2001.

7. A. Taflove (Ed.), *Advances in Computational Electrodynamics: The Finite-Difference Time-Domain Method,* Artech House, Boston, MA, 1998.

8. A. Taflove and S. C. Hagness, *Computational Electrodynamics: The Finite-Difference Time-Domain Method*, Artech House, Boston, MA, 2000.

9. P. J. Dimbylow and S. M. Mann, "SAR Calculations in an Anatomically-Based Realistic Model of the Head for Mobile Communication Transceivers at 900 MHz and 1.8 GHz," *Physics in Med. and Biol.,* Vol. 39**,** pp. 1537-1553, 1994.

10. O. P. Gandhi and J. Y. Chen, "Electromagnetic Absorption in the Human Head from Experimental 6 GHz Handheld Transceivers," *IEEE Trans. on Electromag. Compat.,* Vol. 37, pp. 547-558, 1995.

11. M. A. Jensen and Y. Rahmat-Samii, "EM Interaction in Handset Antennas and a Human in Personal Communications," *Proc. IEEE,* Vol. 83, pp. 7-17, 1995.

12. M. Okoniewski and M. A. Stuchly, "A Study of Handset Antenna and Human Body Interaction, *IEEE Trans. on Microwave Theory and Tech,* Vol.. 44, pp. 1855-1864, 1996.

13. M. A. Stuchly and S. S. Stuchly, "Experimental Radio and Microwave Dosimetry, " in *Handbook of Biological Effects of Electromagnetic Fields,*, 2nd ed., C. Polk and E. Postow, Eds. Boca Raton, FL: CRC, pp. 295-336, 1996.

14. H. I. Bassen and G. S. Smith, "Electric Field Probes -- a Review," *IEEE Trans. Antennas Propagat.,* Vol. AP-31, pp. 710-718, September 1983.

15. D. Hill, "Waveguide Techniques for the Calibration of Miniature Electric Field Probes for Use in Microwave Bioeffects Studies," *IEEE Trans. Microwave Theory Tech.,* Vol. MTT-30, pp. 92-94, 1982.

16. N. Kuster and Q. Balzano, "Energy Absorption Mechanism by Biological Bodies in the Near Field of Dipole Antennas Above 300 MHz," *IEEE Trans. Veh. Technol.,* Vol. 41, pp. 17-23, February 1992.

17. M. A. Stuchly, S. S. Stuchly, and A. Kraszewski, "Implantable Electric Field Probes – Some Performance Characteristics," *IEEE Trans. Biomed. Eng.,* Vol. BME-31, pp. 526-531, July 1984.

18. C. M. Furse, Q. S. Yu, and O. P. Gandhi, "Validation of the Finite-Difference Time-Domain Method for Near-Field Bioelectromagnetic Simulations," *Microwave and Optical Technology Letters*, Vol. 16, pp. 341-345, 1997.

APPENDIX B

EFFECT OF DIELECTRIC PROPERTIES ON THE PEAK 1- AND 10-G SAR FOR 802.11 a/b/g FREQUENCIES 2.45 AND 5.15 TO 5.85 GHz

Gang Kang, Senior Member, IEEE and Om P. Gandhi, Life Fellow, IEEE
Department of Electrical and Computer Engineering
University of Utah
Salt Lake City, Utah 84112, U.S.A.

Abstract

Compliance with 1- or 10-g SAR safety guidelines is required in various countries for all newly-introduced personal wireless devices such as Wi-Fi PCs. Even though the dielectric properties of the human tissues are known to be nonuniform and highly variable, relatively rigid adherence to prescribed dielectric properties (ε_r, σ) is required for compliance testing of such devices. Using some typical near-field irradiators, we have examined the effect of dielectric properties for SAR measurement fluids with conductivities varying by 2:1 to show that both 1- and 10-g SARs vary by less than ± 2-4% for the 802.11a band 5.15 to 5.825 GHz and only slightly more at the lower 802.11 b/g frequency of 2.45 GHz. This is due to higher surface SAR but shallower depth of penetration of EM fields for the higher conductivity media resulting in nearly identical SARs for cubical volumes associated with 1- or 10-g of tissue, respectively. Also studied is the effect of lower ε_r fluids recommended in some standards which results in slightly higher and thus a conservative assessment of SAR.

Accepted for publication in *IEEE Transactions on Electromagnetic Compatibility.*

EFFECT OF DIELECTRIC PROPERTIES ON THE PEAK 1- AND 10-G SAR FOR 802.11 a/b/g FREQUENCIES 2.45 AND 5.15 TO 5.85 GHz

Gang Kang, Senior Member, IEEE and Om P. Gandhi, Life Fellow, IEEE

I. Introduction

Compliance with the safety guidelines such as those proposed by IEEE [1] ICNIRP [2], etc. is required by regulatory agencies in the United States and elsewhere for all newly-introduced personal wireless devices such as Wi-Fi PCs, cellular telephones, etc. These safety guidelines are set in terms of maximum 1- or 10-g mass-normalized rates of electromagnetic energy deposition (specific absorption rates or SARs) for any 1- or 10-g of tissue. The two most commonly-used SAR limits today are those of IEEE [1] – 1.6 W/kg for any 1 g of tissue, and ICNIRP [2] – 2 W/kg for any 10 g of tissue, excluding extremities such as hands, wrists, feet, and ankles where higher SARs up to 4 W/kg for any 10 g of tissue are permitted in both of these standards. Experimental and numerical techniques using planar or head-shaped phantoms have been proposed for determining compliance with the SAR limits [3-5]. Dielectric properties (dielectric constant ε_r and conductivity σ) for the tissue-simulant fluids have been prescribed in three standards based on the properties measured for the various tissues for humans and other mammals [6] and equivalency with the properties needed for a homogeneous planar model to properly represent absorption of incident plane waves to that for a skin-fat-muscle-skull-sclera-CSF-brain layered planar model of a human [7].

In reality, the dielectric properties of the human tissues are highly nonuniform and likely variable with age as well [8]. Thus, dielectric constants and conductivities reported for the various tissues are highly variable and may vary by factors of 2:1 or more for some of the tissues [9]. This paper focuses on the effect of the dielectric properties of the SAR measurement fluids on the peak 1- and 10-g SARs for a planar phantom typically used for compliance testing of wireless PCs and other body- or torso-mounted devices that typically operate at frequencies of 2.4-2.484 GHz (802.11 b/g systems) and in the 5 GHz band for frequencies of 5.15 to 5.35 and 5.745 to 5.825 GHz (802.11a systems). For a 2:1 or 100% variability in conductivity of the tissue-simulant fluid, the variation in peak 1- and 10-g SAR is less than ± 2-4% for the higher frequency band 5.15 to 5.825 GHz and only slightly higher for the lower 802.11 b/g wireless systems band of 2.45 GHz. The reason for this is the higher surface SAR but shallower depth of penetration of electromagnetic fields for the higher conductivity media which has the net effect of providing nearly identical SAR for volumes in the shape of a cube, of dimensions 1 or 2.154 cm associated with 1- or 10-g of tissue, respectively. Though relatively negligible at 2.45 GHz, it is shown that the effect of the changing dielectric constant ε_r (instead of conductivity) is somewhat larger on both 1- and 10-g SARs for the 5-6 GHz band with the lower ε_r phantom materials resulting in 10-12 percent higher SARs. Thus the lower ε_r media recommended by IEC PT62209 [5] for the 5-6 GHz band may be used if a conservative determination of SAR is of interest.

II. Assumed EM Sources

The sources of microwave radiation typically used in wireless PCs are one or two dual band microstrip antennas either fabricated on an insertable wireless card or built into the base or at times behind the display screen of the PC. A wide variety of antenna dimensions and

locations are typically used. For the purpose of calculations of peak 1- or 10-g SARs, we have assumed a typical microstrip antenna (see Fig. 1) and a couple of additional sources of EM radiation that are recommended in the compliance standards [3-5] for SAR measurement system validation. The three EM sources thus selected are: a square microstrip antenna of dimensions 30 × 30 mm placed with a spacing of 4 mm above a ground plane of dimensions 40 × 40 mm, a nominal half wave dipole of length 51.5 mm and diameter 3.6 mm recommended for 2.45 GHz in [3, 4] and a WR187 open-ended rectangular waveguide of internal dimensions 4.75 × 2.21 cm that may be used in the frequency band 5.1 to 5.8 GHz for SAR system validation. As recommended in the compliance standards [3-5], these sources are assumed to be placed under a planar phantom of a relatively thin base of thickness 2.0 mm made of a lossless dielectric and of sufficiently large lateral dimensions to be able to ignore scattering from the edges of the planar box or the tissue-simulant lossy fluid used to fill this box to a depth of 15 cm (several times the depth of penetration of fields in the fluid so as to present a nearly infinitely deep medium to neglect reflections). For the present calculations using the finite-difference time-domain (FDTD) numerical technique, we have used a planar phantom box of inside dimensions 30.5 × 41.9 × 20 cm made of acrylic ($\varepsilon_r = 2.56$) of base thickness 2.0 mm that is assumed to be filled with a tissue-simulant fluid of different dielectric properties (ε_r, σ) up to a depth of 15 cm. As recommended in the compliance standards [3-5], each of the three aforementioned sources of EM fields; namely, the microstrip antenna, the half-wave dipole or the open-ended rectangular waveguide, are assumed to be placed at a distance of 8.0 mm below the base of the planar phantom, resulting in a separation of 10 mm to the bottom level of the tissue-simulant fluid. A microstrip antenna is generally mounted in the base of a wireless portable computer (PC) which is tested for above-lap placement for one of the configurations. Thus, the ground plate of dimensions 40 × 40 mm for the assumed microstrip antenna is placed at a distance of 8 mm below the base of the planar phantom. The microstrip of dimensions 30 × 30 mm is assumed to be printed on a substrate of dielectric constant $\varepsilon_r = 2.56$ and thickness 4 mm.

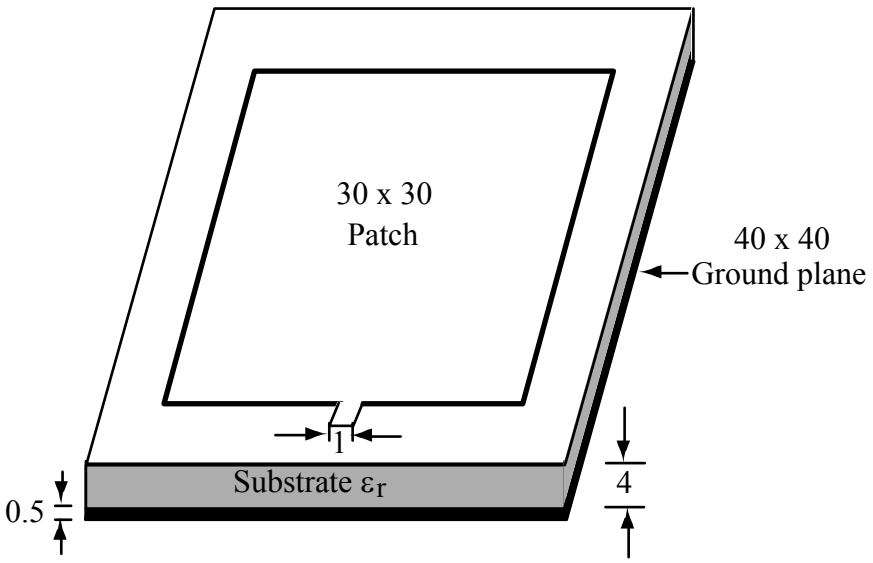

Fig. 1. A square patch microstrip antenna typical of wireless PCs. All dimensions are in mm.

III. The Finite-Difference Time-Domain Method

The method used for SAR distributions is the well-established finite-difference time-domain (FDTD) method. This method described in several texts [10, 11] has been used successfully by various researchers [12-15] and, therefore, would not be described here in any detail. For the FDTD calculations, we used a cell size 0.5 × 0.5 × 0.5 mm both at 2.45 GHz and for the two representative frequencies of 5.25 and 5.80 GHz in the 5-6 GHz band. This was done to meet the requirement $\delta \leq \lambda_\varepsilon / 10$ in the lossy tissue-simulant fluid as well as in recognition of the fact that the depth of penetration δ_s in the fluid is fairly small being on the order of 13-26 mm at 2450 MHz and less than 5-9 mm for the 5 GHz band. The dielectric properties (ε_r, σ) assumed for the "tissue-simulant" fluids for the two calculation bands are those given in the various compliance standards and conductivities that are 75% or 150% of those suggested in the various standards [3-5].

The values of ε_r, σ taken for various frequencies are given in Table 1. The dielectric properties are those suggested by the FCC OET Bulletin 65 Supplement C [16] and IEC TC 106/PT62209 [5] and SAR measurement fluids that may have conductivities that are 0.75 or 1.5 times those suggested for the flat body-simulant phantom in [5, 16]. Thus a 2:1 variation of conductivities is assumed for the SAR measuring fluid of the flat phantom.

IV. Calculated 1- and 10-g SARs

As recommended in the IEEE [1] and CENELEC [4] Standards, the peak 1- and 10-g SARs are calculated using cubes of dimensions 10 or 21.5 mm, respectively. Given in Tables 1 and 2 also are the peak 1- or 10-g SARs thus calculated for the various tissue-simulant fluids and several near-field irradiation systems at a number of frequencies typical of Wi-Fi PCs. Important points to note from the results of Tables 1 and 2 are as follows:

1. For a 2:1 variation in conductivity of the tissue-simulant fluids, the variation in peak 1- and 10-g SARs is within ± 2-4% for frequencies in the 802.11a 5 GHz band e.g. 5.25 and 5.8 GHz. The variation in peak 1- or 10-g SAR is higher at the lower frequency of 2.45 GHz. However, there is a move to harmonize the various compliance standards in terms of the peak 10- rather than 1-g SARs. For a 2:1 variation in the conductivity, the variation in peak 10-g SAR at 2.45 GHz is within ± 10%.

2. The effect of lower dielectric constant ε_r recommended by IEC PT62209 [5] is relatively small at 2.45 GHz (≤ 4 %) but is somewhat higher for the 5-6 GHz band. Both the 1- and 10-g SARs are higher by up to 10-12 percent for the 5 GHz band for the lower dielectric constant tissue-simulant fluids recommended by IEC PT62209 [5] as compared to those suggested in FCC OET Bulletin 65 [14].

The result of a relatively negligible variation of peak 1- and 10-g SAR in spite of a 2:1 change in conductivity is very surprising, since as expected, there is a highly variable penetration of EM energy into the different conductivity tissue-simulant fluids as seen in Tables 1, 2 and Figs. 2-5, respectively. As expected, somewhat deeper penetration is observed for lower

conductivity fluids and increasingly shallower penetration is observed as the conductivity is increased both at 2.45 GHz and at frequencies in the 5-6 GHz band (see Tables 1, 2). Also to be noticed in Figs. 2-5 are the higher surface SARs for the higher conductivity fluids which tend to compensate for the shallower penetration of fields in such fluids. This is the reason for relatively constant 1- and 10-g SARs in spite of the wide variation of the conductivity of the media.

Table 1. Assumed dielectric properties (ε_r , σ) taken for frequencies 2.45, 5.25, and 5.80 GHz and the FDTD-calculated peak 1- and 10-g SARs for some typical near-field radiators. The irradiators are assumed to be placed 10 mm below the bottom surface of the tissue-simulant fluid in a flat phantom of base thickness 2 mm with (ε_r = 2.56). Radiated Power = 100 mW.

Frequency GHz	Near Field Radiator	Assumed Dielectric Properties			$1/e^2$ Depth of Power Penetration (mm)	1-g SAR (W/kg)	10-g SAR (W/kg)
		ε_r	σ (S/m)	Reference			
2.45	Dipole	52.7	1.46	Lower σ @ 75% of FCC	18.1	4.34	2.12
			1.95	FCC, body [16]	14.6	5.13	2.32
			2.93	Higher σ @ 150% of FCC	10.7	6.13	2.48
		39.2	1.35	Lower σ @ 75% of IEC	16.9	4.41	2.16
			1.80	IEC/FCC, head [5]	13.7	5.18	2.35
			2.70	Higher σ @ 150% of IEC	10.1	6.14	2.49
5.25	Waveguide	48.9	4.02	Lower σ @ 75% of FCC	8.9	3.37	1.44
			5.36	FCC, body [16]	6.8	3.57	1.44
			8.04	Higher σ @ 150% of FCC	4.6	3.63	1.42
		35.9	3.53	Lower σ @ 75% of IEC	8.7	3.79	1.61
			4.71	IEC/FCC, head [5]	6.7	3.99	1.61
			7.07	Higher σ @ 150% of IEC	4.6	4.02	1.57
5.80	Waveguide	48.2	4.50	Lower σ @ 75% of FCC	7.9	3.79	1.59
			6.00	FCC, body [16]	6.0	3.95	1.58
			9.00	Higher σ @ 150% of FCC	4.1	3.94	1.54
		35.3	3.95	Lower σ @ 75% of IEC	7.7	4.26	1.77
			5.27	IEC/FCC, head [5]	5.9	4.42	1.76
			7.91	Higher σ @ 150% of IEC	4.1	4.36	1.70

Table 2. Assumed dielectric properties (ε_r, σ) taken for frequencies 2.45, 5.25, and 5.80 GHz and the FDTD-calculated peak 1- and 10-g SARs for a typical microstrip antenna of dimensions 30 × 30 mm placed 4 mm above a ground plane of dimensions 40 × 40 mm (see Fig. 1). As required by the compliance standards [5, 16], the ground plane of the microstrip antenna is assumed to be 10 mm below the bottom surface of the tissue-simulant fluid (microstrip at 14.5 mm below the fluid). Radiated Power = 100 mW.

Frequency GHz	Assumed Dielectric Properties		$1/e^2$ Depth of Power Penetration (mm)	1-g SAR (W/kg)	10-g SAR (W/kg)
	ε_r	σ (S/m)			
2.45	52.7	1.46	25.2	2.26	1.43
		1.95	19.0	2.71	1.57
		2.93	13.2	3.37	1.72
	39.2	1.35	23.4	2.36	1.47
		1.80	18.3	2.82	1.61
		2.70	11.6	3.60	1.77
5.25	48.9	4.02	9.2	1.52	0.52
		5.36	7.0	1.60	0.51
		8.04	4.7	1.62	0.50
	35.9	3.53	9.0	1.57	0.53
		4.71	6.8	1.64	0.53
		7.07	4.6	1.66	0.51
5.80	48.2	4.50	8.0	1.96	0.57
		6.00	6.0	2.03	0.56
		9.00	4.1	2.03	0.54
	35.3	3.95	7.7	2.03	0.60
		5.27	5.9	2.10	0.59
		7.91	4.1	2.09	0.56

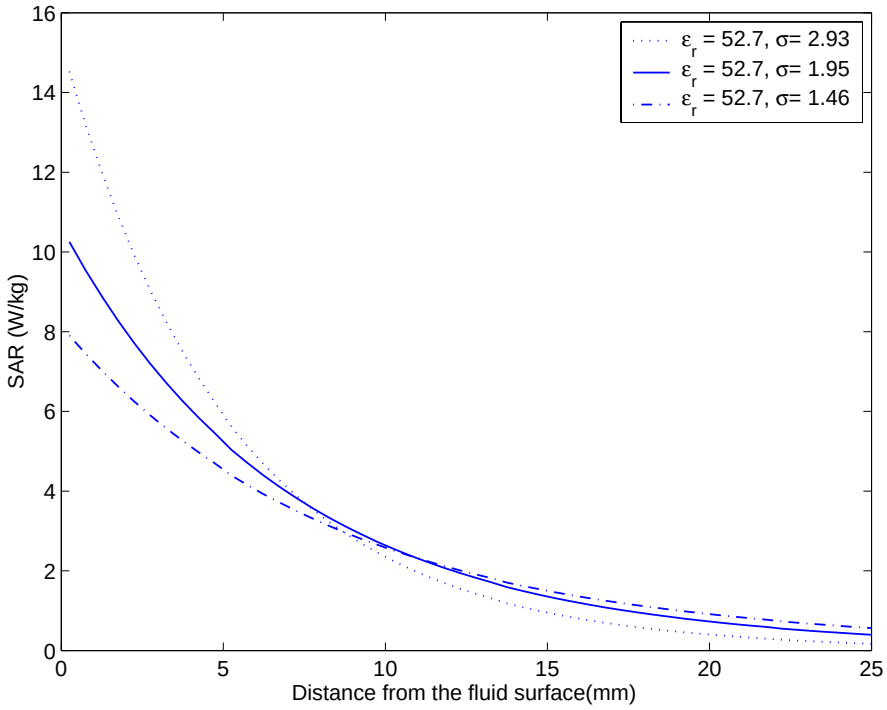

Fig. 2. **The dipole antenna.** Comparison of the FDTD-calculated variation of the SAR with depth for the various tissue-simulant media at 2.45 GHz.

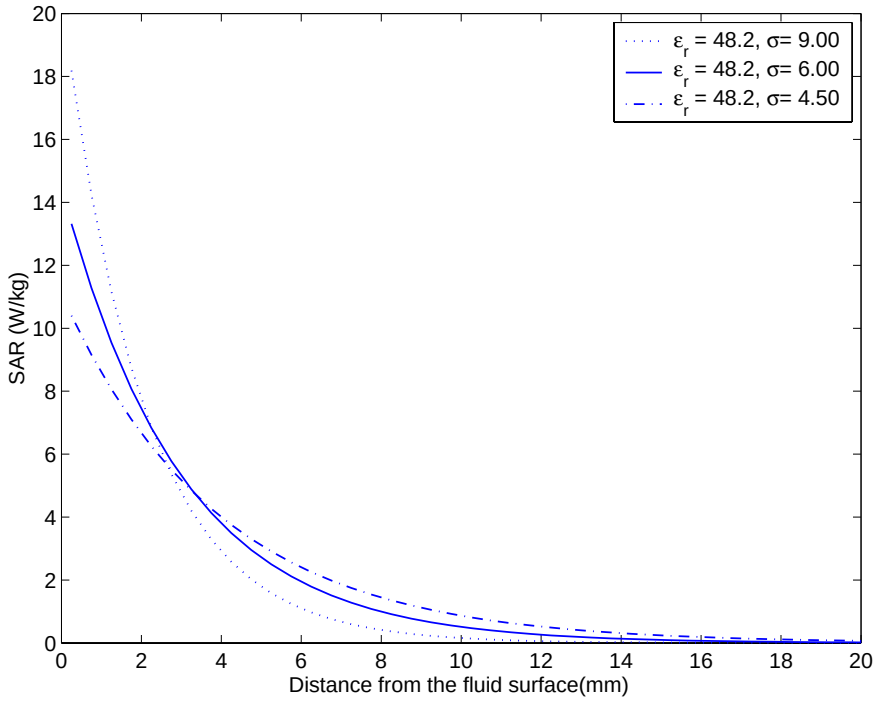

Fig. 3. **The rectangular waveguide radiator.** Comparison of the FDTD-calculated variation of the SAR with depth for the various tissue-simulant media at 5.8 GHz.

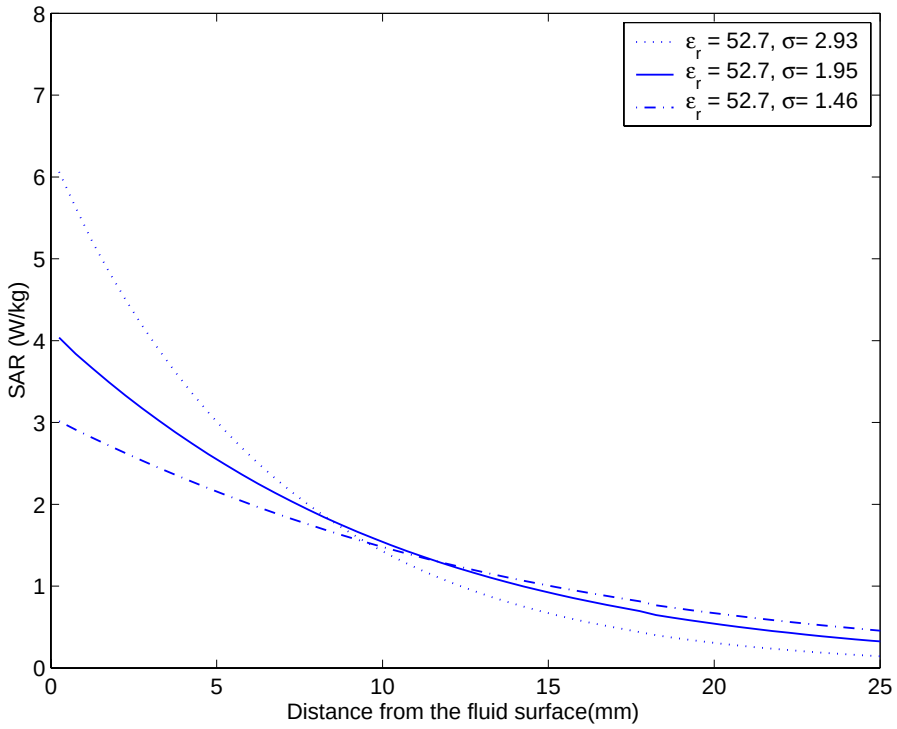

Fig. 4. **The microstrip antenna.** Comparison of the FDTD-calculated variation of the SAR with depth for the various tissue-simulant media at 2.45 GHz.

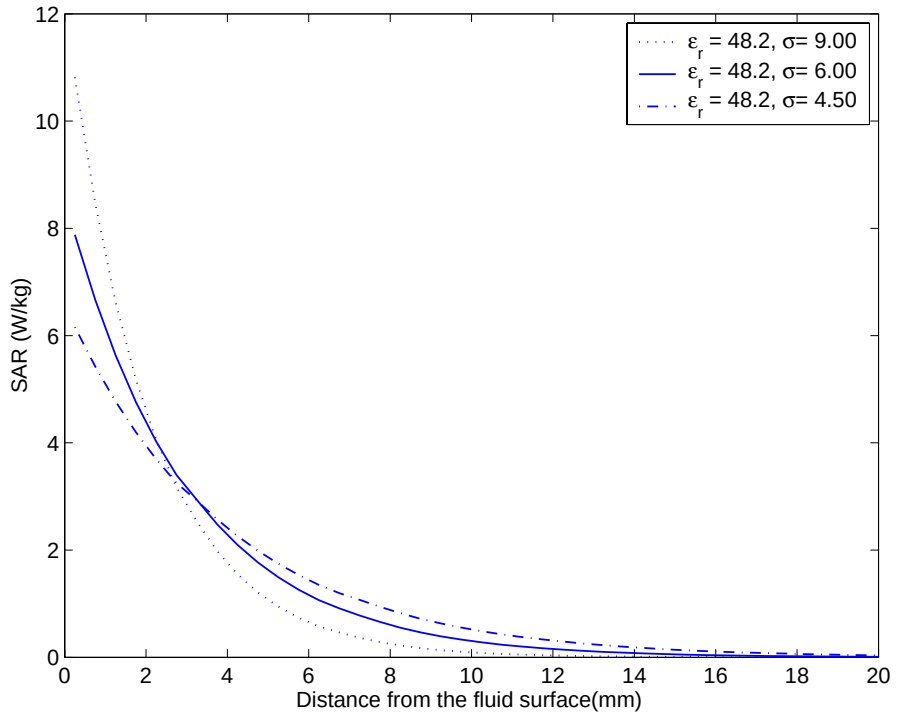

Fig. 5. **The microstrip antenna.** Comparison of the FDTD-calculated variation of the SAR with depth for the various tissue-simulant media at 5.8 GHz.

V. Comparison with Plane Wave Exposures

The above results are easy to understand when one looks at the peak 1- and 10-g SARs for plane waves incident normally at a semi-infinite slab of tissue-simulant fluid of variable dielectric properties. Given in Table 3 are some of the salient parameters and the peak 1- and 10-g SARs calculated for plane waves that are incident normal to a semi-infinite slab of dielectric properties similar to those of tissue-simulant media. Unlike the case of near-field exposure systems in Tables 1 and 2, closed-form analytical expressions given in the following may be used for this case of plane waves.

Table 3. Calculated skin depths, power transmission coefficients, and peak 1- and 10-g SARs for plane waves of power density 1 mW/cm^2 for normal incidence on a semi-infinite slab of tissue-simulant media of different assumed dielectric properties at 2.45, 5.25 and 5.80 GHz.

Frequency GHz	Assumed Dielectric Properties		Skin Depth (mm)	Power Transmission Coefficient TT*	1-g SAR (W/kg)	10-g SAR (W/kg)
	ε_r	σ (S/m)				
2.45	52.7	1.46	26.5	0.42	0.22	0.16
		1.95	19.9	0.42	0.26	0.17
		2.93	13.4	0.41	0.32	0.18
	39.2	1.35	24.8	0.47	0.26	0.18
		1.80	18.7	0.46	0.30	0.19
		2.70	12.7	0.45	0.35	0.20
5.25	48.9	4.02	9.3	0.43	0.38	0.20
		5.36	7.0	0.42	0.40	0.20
		8.04	4.8	0.41	0.40	0.19
	35.9	3.53	9.1	0.48	0.42	0.22
		4.71	6.9	0.47	0.44	0.22
		7.07	4.7	0.44	0.44	0.22
5.80	48.2	4.50	8.3	0.43	0.39	0.20
		6.00	6.3	0.42	0.41	0.20
		9.00	4.3	0.41	0.40	0.19
	35.3	3.95	8.1	0.48	0.44	0.22
		5.27	6.1	0.47	0.45	0.22
		7.91	4.2	0.44	0.44	0.21

For a lossy slab of dielectric constant ε_r and conductivity σ, the complex dielectric constant ε^* at radian frequency ω can be written as:

$$\varepsilon^* = \varepsilon_r - j\frac{\sigma}{\omega\varepsilon_o} = \varepsilon_r - j\varepsilon'' \tag{1}$$

The propagation constant γ in the lossy medium can be written as $\gamma = \alpha + j\beta$ where the attenuation constant α and propagation constant β can be written as follows [17]:

$$\alpha = \omega\sqrt{\frac{\mu\varepsilon_o\varepsilon_r}{2}}\left[\sqrt{1+\left(\frac{\varepsilon''}{\varepsilon_r}\right)^2} - 1\right]^{1/2} \tag{2}$$

$$\beta = \omega\sqrt{\frac{\mu\varepsilon_o\varepsilon_r}{2}}\left[\sqrt{1+\left(\frac{\varepsilon''}{\varepsilon_r}\right)^2} + 1\right]^{1/2} \tag{3}$$

The skin depth δ_s is given by $1/\alpha$ and the complex reflection coefficient ρ at the air-slab interface is given by

$$\rho = \frac{1-\sqrt{\varepsilon^*}}{1+\sqrt{\varepsilon^*}} \tag{4}$$

The power transmission coefficient is given by $TT^* = (1-\rho\rho^*)$.

For an incident power density S_{inc} mW/cm^2, the peak 1- and 10-g SARs in mW/g or W/kg are given by the following equations:

$$\text{Peak 1-g SAR} = \left[1-e^{-2/\delta_s}\right]\left(TT^*\right)S_{inc} \qquad \text{W/kg} \tag{5}$$

$$\text{Peak 10-g SAR} = \frac{4.64}{10}\left[1-e^{-4.309/\delta_s}\right]\left(TT^*\right)S_{inc} \qquad \text{W/kg} \tag{6}$$

As for the case of the assumed near-field irradiators, here too, the results are very similar with an advantage that a physical insight into the results is now possible.

1. For a 2:1 increase in conductivity of the SAR measurement fluid, the variation in peak 10-g SAR is relatively small and generally within ± 2.5% for all of the frequencies in the band 5.25 to 5.8 GHz (see Table 3). However, for the lower frequency of 2.45 GHz, there is a somewhat higher variation in peak 1-g SAR (± 23%) and a considerably lower variation on the order of ± 5-6% for the peak 10-g SAR. The reason for such a small variation is that the power transmission coefficient varies very little with conductivity of the fluid particularly for the higher dielectric constant media. All of the power thus coupled into the tissue-simulant medium is absorbed by the 10-g averaging volume, particularly for the 5-6 GHz band, since the depth of penetration is only on the order of 4-

9 mm as seen in Table 3. In fact, the peak 10-g SAR given in the last column of Table 3 at the higher frequencies of 5.25 and 5.8 GHz is nothing but the power coupled into a surface area of 2.154 cm × 2.154 cm or 4.64 cm^2 divided by 10 g.

2. Similar to the cases of the near-field irradiators of Tables 1 and 2, the peak 1- and 10-g SARs for plane waves for the lower dielectric constant (ε_r) media recommended by IEC TC 106/PT62209 are slightly higher than those for the higher ε_r media recommended in FCC OET Bulletin 65 [16]. As seen in Table 3, this is due to somewhat higher power transmission coefficients for the media with lower dielectric constants.

VI. Conclusions

We have examined the effect of dielectric properties (ε_r, σ) of SAR measuring tissue-simulant media on the peak 1- and 10-g SARs both for near-field sources and for plane waves since the dielectric properties reported for the various tissues are highly variable. For a 2:1 variability in the conductivity of tissue-simulant fluid, the variation in peak 1- and 10-g SAR is negligible within ± 2-4% for the 5 to 6 GHz band and only slightly larger on the order of ± 10% for the 2.45 GHz band, particularly for the all-important 10-g SAR. Thus, an exact match to the conductivities or the dielectric constant recommended in the various compliance standards is not really necessary as far as determination of 1- or 10-g SARs is concerned. This is important since tissue dielectric properties are known to be highly nonuniform and considerably variable between individuals [9]. Both the 1- and 10-g SARs are, however, higher by about 10-12% for the lower ε_r media recommended by IEC TC 106/PT62209 [5], which may, therefore, be used if a conservative determination of SAR is of interest.

REFERENCES

1. IEEE Std. C95.1, "IEEE Standard for Safety Levels with Respect to Human Exposure to Radiofrequency Electromagnetic Fields, 3 kHz to 300 GHz," Institute of Electrical and Electronics Engineers, Piscataway, NJ, 1999.

2. ICNIRP (International Commission on Non-Ionizing Radiation Protection), "Guidelines for limiting exposure to time-varying electric, magnetic, and electromagnetic fields (up to 300 GHz)", *Health Physics*, Vol. 74, pp. 494-522, 1998.

3. IEEE Standards Coordinating Committee 34, "Recommended Practice for Determining the Peak Spatial-Average Specific Absorption Rate (SAR) in the Human Body Due to Wireless Communications Devices: Experimental Techniques," Institute of Electrical and Electronics Engineers, Draft Standard, 2003.

4. CENELEC EN50361, "Basic Standard for Measurement of Specific Absorption Rate Related to Human Exposure to Electromagnetic Fields from Mobile Telephones (300-MHz-3 GHz), CENELEC European Committee for Electrotechnical Standardization, rue de Stassart 35, B-1050, Brussels, Belgium, 2001.

5. IEC TC 106/PT62209, "Evaluation of Human Exposure to Radiofrequency Fields from Handheld and Body-Mounted Wireless Communications Devices in the Frequency Range of 30 MHz to 6 GHz: Human Models, Instrumentation Procedures," Draft Standard in preparation, 2003.

6. C. Gabriel, "Compilation of the Dielectric Properties of Body Tissues at RF and Microwave Frequencies," Report AL/OE-TR-1996-0037, Armstrong Laboratory (AFMC), Radiofrequency Radiation Division, Brooks AFB, TX (www.brooks.af.mil/AFRL/HED/hedr/reports/dielectric/home.html).

7. A. Drossos, V. Santomaa, and N. Kuster, "The Dependence of Electromagnetic Energy Absorption Upon Human Head Tissue Composition in the Frequency Range of 300-3000 MHz," *IEEE Transactions on Microwave Theory and Techniques,* Vol. 48(11), pp. 1988-1995, November 2000.

8. A Peyman, A. A. Rezazadeh, and C. Gabriel, "Changes in the Dielectric Properties of Rat Tissue as a Function of Age at Microwave Frequencies," *Physics in Medicine and Biology,* Vol. 46, pp. 1617-1629, 2001.

9. M. A. Stuchly and S. S. Stuchly, "Dielectric Properties of Biological Substances – Tabulated," *Jour. Microwave Power*, Vol. 15, pp. 19-26, 1980.

10. A. Taflove (Ed.), *Advances in Computational Electrodynamics: The Finite-Difference Time-Domain Method,* Artech House, Boston, MA, 1998.

11. A. Taflove and S. C. Hagness, *Computational Electrodynamics: The Finite-Difference Time-Domain Method*, Artech House, Boston, MA, 2000.

12. P. J. Dimbylow and S. M. Mann, "SAR Calculations in an Anatomically-Based Realistic Model of the Head for Mobile Communication Transceivers at 900 MHz and 1.8 GHz," *Physics in Med. and Biol.,* Vol. 39**,** pp. 1537-1553, 1994.

13. O. P. Gandhi and J. Y. Chen, "Electromagnetic Absorption in the Human Head from Experimental 6 GHz Handheld Transceivers," *IEEE Trans. on Electromag. Compat.,* Vol. 37, pp. 547-558, 1995.

14. M. A. Jensen and Y. Rahmat-Samii, "EM Interaction in Handset Antennas and a Human in Personal Communications," *Proc. IEEE,* Vol. 83, pp. 7-17, 1995.

15. M. Okoniewski and M. A. Stuchly, "A Study of Handset Antenna and Human Body Interaction, *IEEE Trans. on Microwave Theory and Tech,* Vol.. 44, pp. 1855-1864, 1996.

16. U.S. Federal Communications Commission (FCC), Supplement C (Edition 01-01) to OET Bulletin 65 (Edition 97-01), "Additional Information for Evaluating Compliance of Mobile and Portable Devices with FCC Limits for Human Exposure to Radiofrequency Radiation," June 2001 (www.fcc.gov/oet/info/documents/bulletins/#65)

17. C. A. Balanis, *Advanced Engineering Electromagnetics,* John Wiley & Sons, 1989.

APPENDIX C

1. PEAK TRANSMIT POWER MEASUREMENT

2. LIMITS OF PEAK TRANSMIT POWER MEASUREMENT

Frequency Band	Limit
5.15 – 5.25GHz	The lesser of 50mW (17dBm) or 4dBm + 10logB
5.25 – 5.35GHz	The lesser of 250mW (24dBm) or 11dBm + 10logB
5.725 – 5.825GHz	The lesser of 1W (30dBm) or 17dBm + 10logB

Note: Where B is the 26dB emission bandwidth in MHz.

3. TEST INSTRUMENTS

Description & Manufacturer	Model No.	Serial No.	Calibrated Until
SPECTRUM ANALYZER	FSEK30	100049	July 24, 2003

NOTE: The calibration interval of the above test instruments is 12 months and the calibrations are traceable to NML/ROC and NIST/USA.

4. TEST PROCEDURE

1. The transmitter output was connected to the spectrum analyzer.
2. Set span to encompass the entire emission bandwidth of the signal.
3. Set RBW to 1MHz, VBW to 300kHz.
4. Using the spectrum analyzer's channel power measurement function to measure the output power.

5. DEVIATION FROM TEST STANDARD

No deviation

6. TEST SETUP

7. EUT OPERATING CONDITIONS

The software provided by client to enable the EUT under transmission condition continuously at specific channel frequencies individually.

8. TEST RESULTS

EUT	Wireless Cardbus Adapter	**MODEL**	SL-5354CB ARIES
ENVIRONMENTAL CONDITIONS	25deg. C, 68%RH, 991hPa	**INPUT POWER (SYSTEM)**	120Vac, 60 Hz
TESTED BY	Ansen Lei		

CHANNEL	CHANNEL FREQUENCY (MHz)	PEAK POWER OUTPUT (dBm)	PEAK POWER LIMIT (dBm)	26dBc Occupied Bandwidth (MHz)	PASS/FAIL
1	5180	14.85	17.00	33.43	PASS
4	5240	14.64	17.00	34.79	PASS
5	5260	14.62	24.00	35.51	PASS
8	5320	14.82	24.00	37.27	PASS
9	5745	18.43	30.00	42.08	PASS
12	5805	18.87	30.00	43.79	PASS

NOTE: The 26dBc Occupied Bandwidth plot, please refer to the following pages.

CHANNEL 1

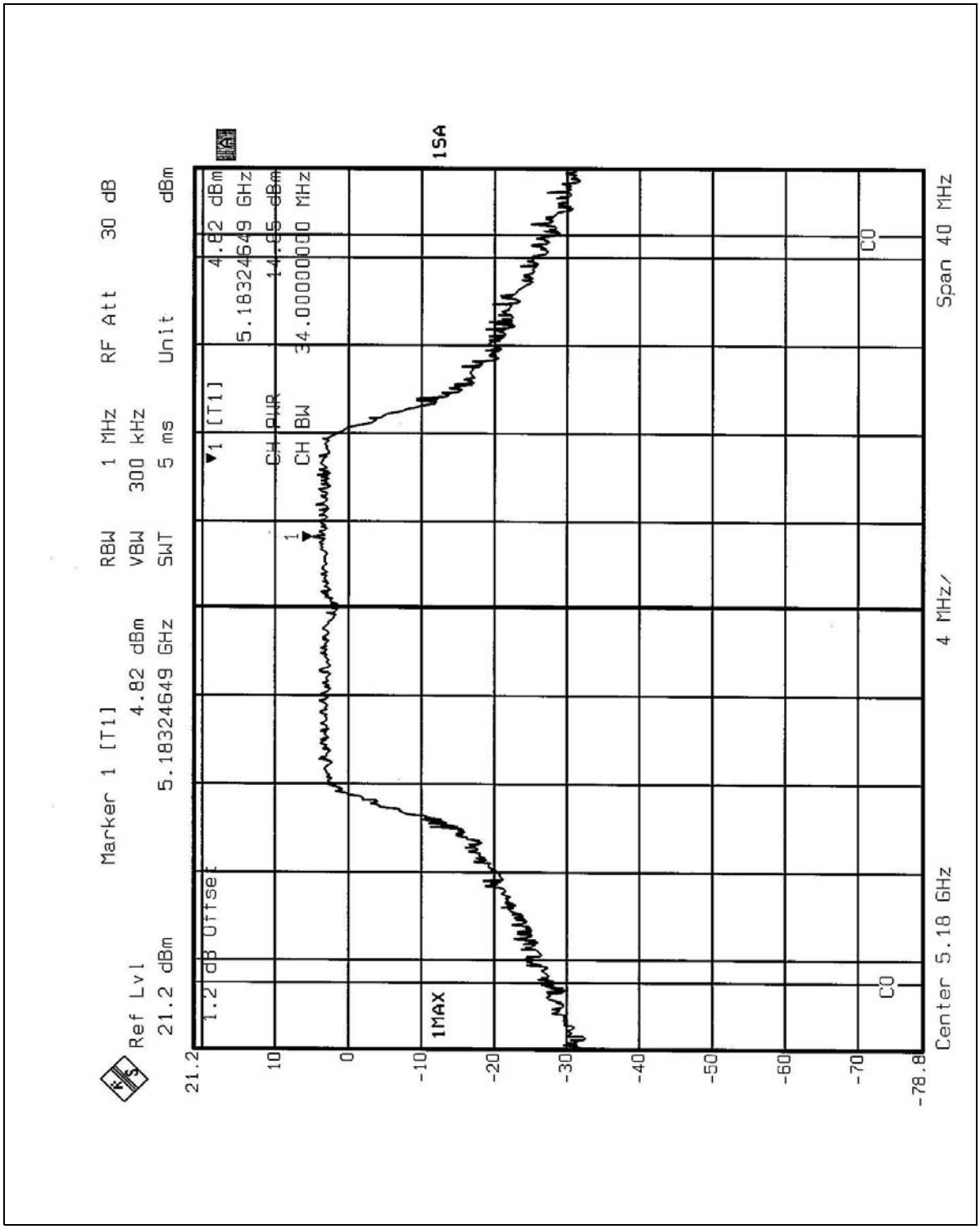
Marker 1 [T1]
4.82 dBm
5.18324649 GHz
Ref Lvl
21.2 dBm
1.2 dB Offset
RBW 1 MHz
VBW 300 kHz
SWT 5 ms
RF Att 30 dB
Unit dBm
1 [T1]
4.82 dBm
5.18324649 GHz
CH PWR 14.05 dBm
CH BW 34.000000000 MHz
1SA
1MAX
Center 5.18 GHz
4 MHz/
Span 40 MHz

CHANNEL 4

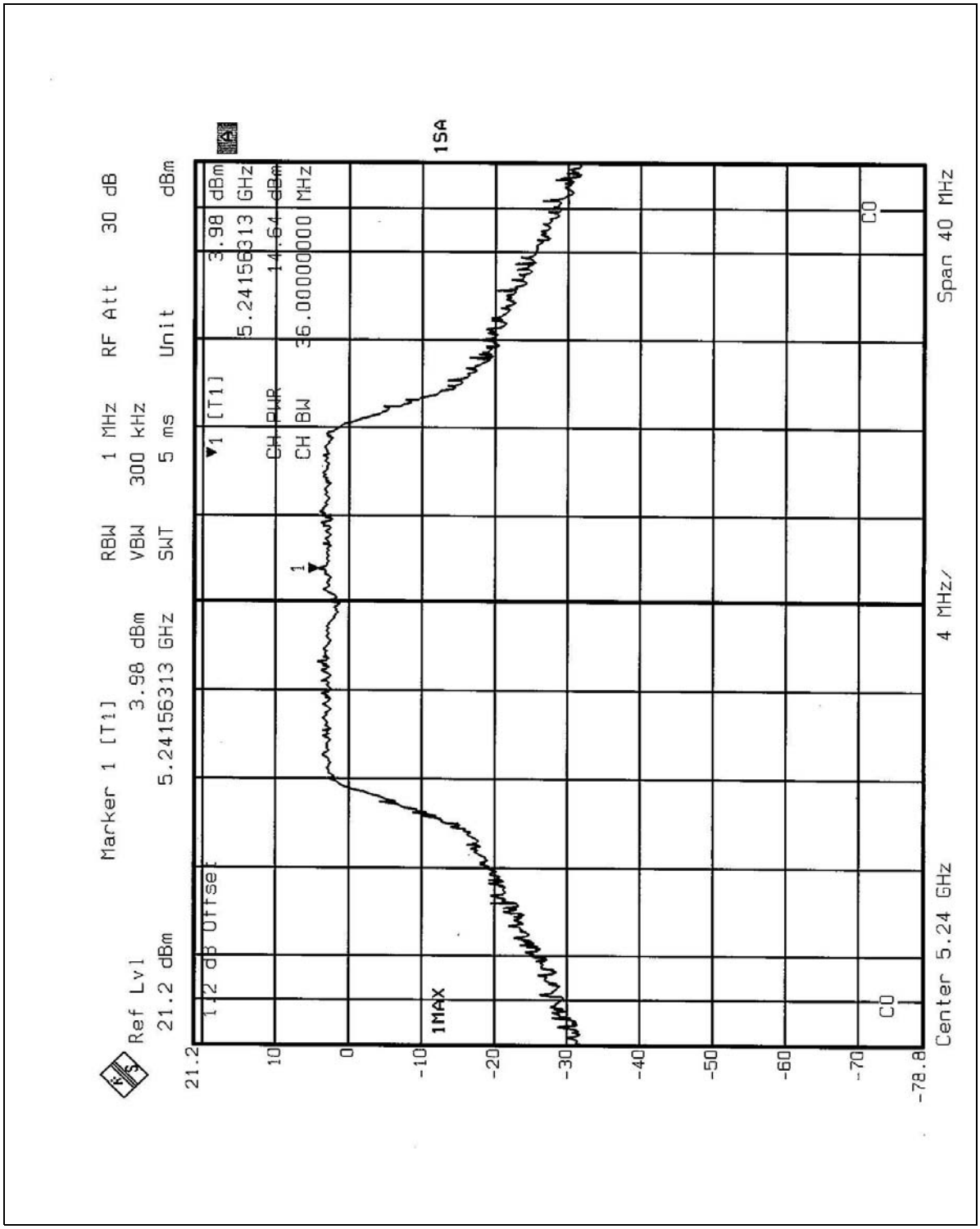
Marker 1 [T1]
3.98 dBm
5.24156313 GHz
Ref Lvl
21.2 dBm
RBW 1 MHz
VBW 300 kHz
SWT 5 ms
RF Att 30 dB
Unit dBm
1 [T1]
3.98 dBm
5.24156313 GHz
CH PWR 14.64 dBm
CH BW 36.000000000 MHz
1SA
1MAX
Center 5.24 GHz
4 MHz/
Span 40 MHz

CHANNEL 5

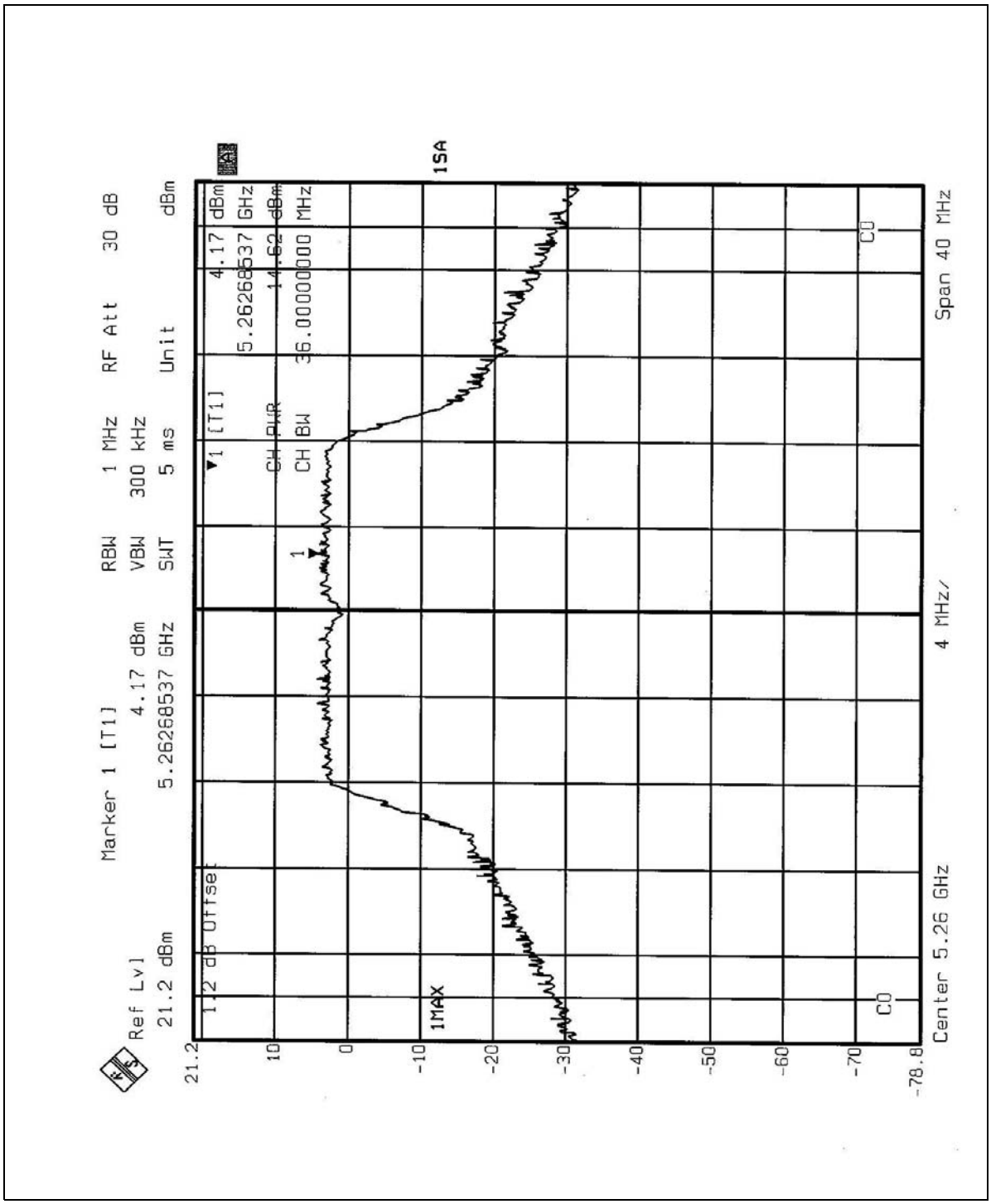
Marker 1 [T1]
4.17 dBm
5.26268537 GHz
Ref Lvl
21.2 dBm
RBW 1 MHz
VBW 300 kHz
SWT 5 ms
RF Att 30 dB
Unit dBm
1SA
1 [T1]
4.17 dBm
5.26268537 GHz
CH PWR 14.62 dBm
CH BW 36.00000000 MHz
1 12 dB Offset
1MAX
Center 5.26 GHz
4 MHz/
Span 40 MHz

CHANNEL8

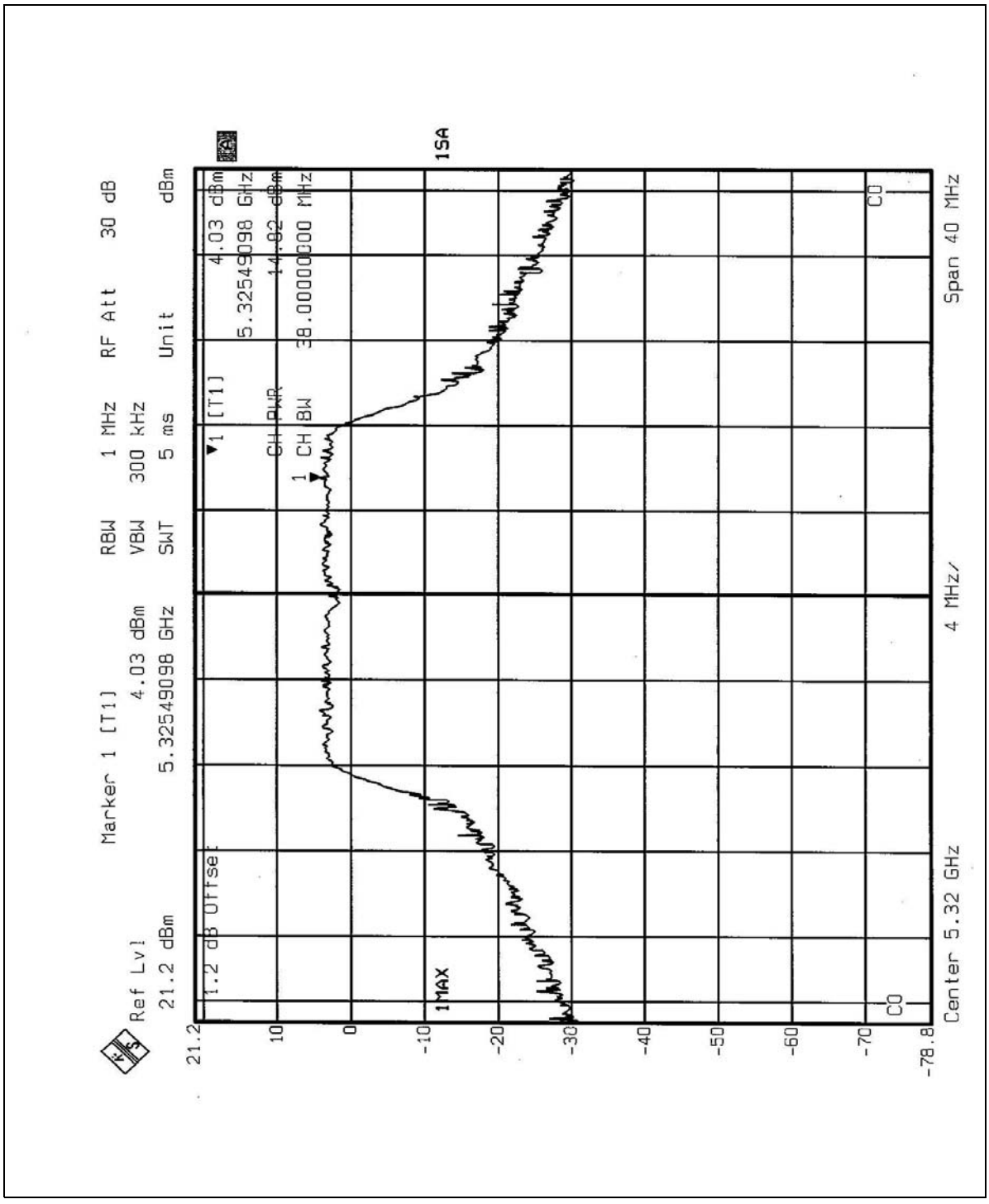
Ref Lvl
21.2 dBm
1.2 dB Offset
Marker 1 [T1]
4.03 dBm
5.32549098 GHz
RBW 1 MHz
VBW 300 kHz
SWT 5 ms
RF Att 30 dB
Unit dBm
1SA
1 [T1]
4.03 dBm
5.32549098 GHz
CH PWR 14.82 dBm
1 CH BW 38.00000000 MHz
1MAX
21.2
10
0
-10
-20
-30
-40
-50
-60
-70
-78.8
Center 5.32 GHz
4 MHz/
Span 40 MHz

CHANNEL9

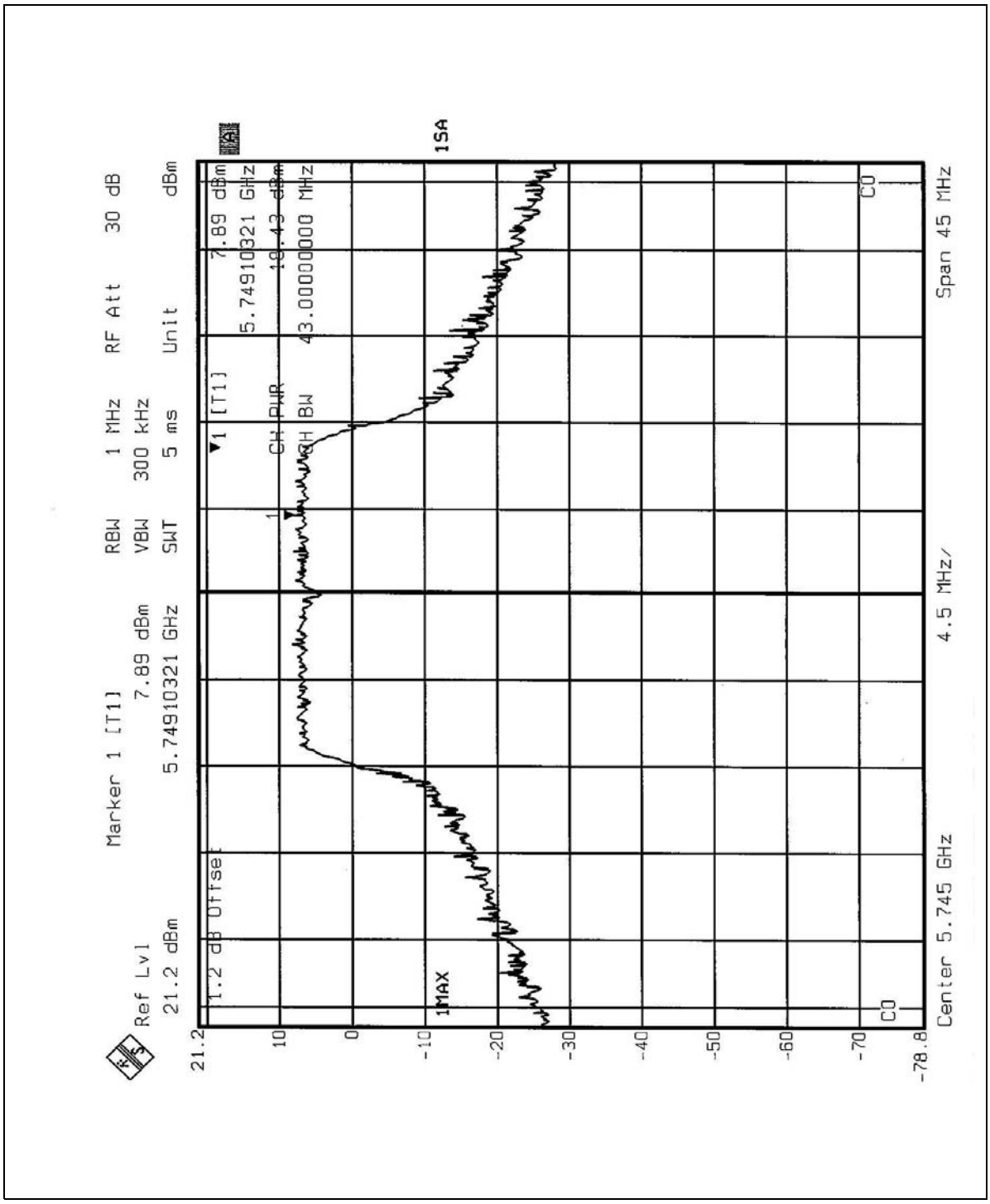
Marker 1 [T1]
7.89 dBm
5.74910321 GHz
Ref Lvl
21.2 dBm
1.2 dB Offset
RBW 1 MHz
VBW 300 kHz
SWT 5 ms
RF Att 30 dB
Unit dBm
1 [T1]
7.89 dBm
5.74910321 GHz
CH PWR 19.43 dBm
CH BW 43.000000000 MHz
1SA
1MAX
Center 5.745 GHz
4.5 MHz/
Span 45 MHz
21.2
10
0
-10
-20
-30
-40
-50
-60
-70
-78.8

CHANNEL12

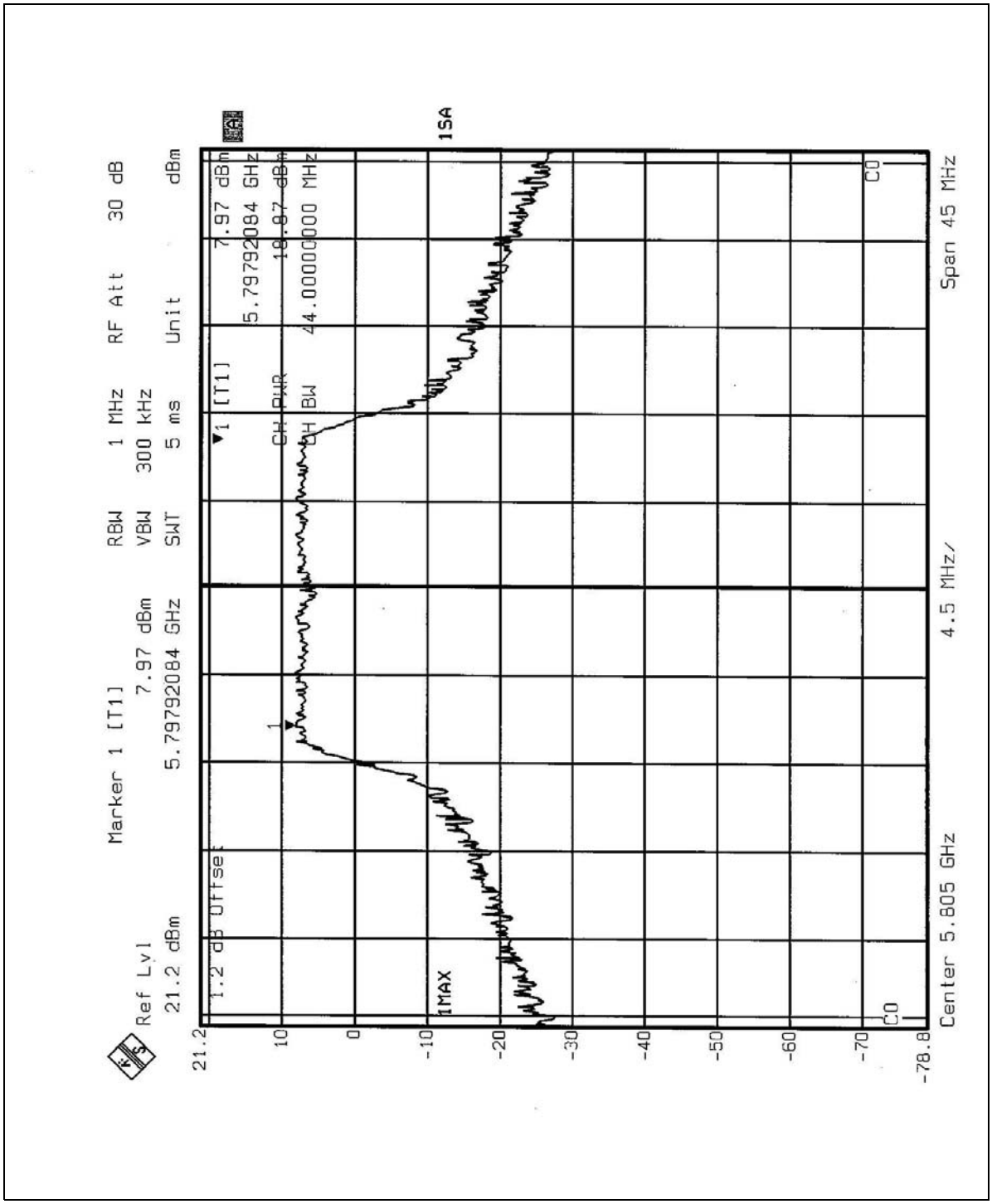
Ref Lvl
21.2 dBm
1.2 dB Offset
Marker 1 [T1]
7.97 dBm
5.79792084 GHz
RBW 1 MHz
VBW 300 kHz
SWT 5 ms
RF Att 30 dB
Unit dBm
1 [T1]
7.97 dBm
5.79792084 GHz
CH PWR 18.87 dBm
CH BW 44.00000000 MHz
1SA
1MAX
21.2
10
0
-10
-20
-30
-40
-50
-60
-70
-78.8
Center 5.805 GHz
4.5 MHz/
Span 45 MHz

CHANNEL 1

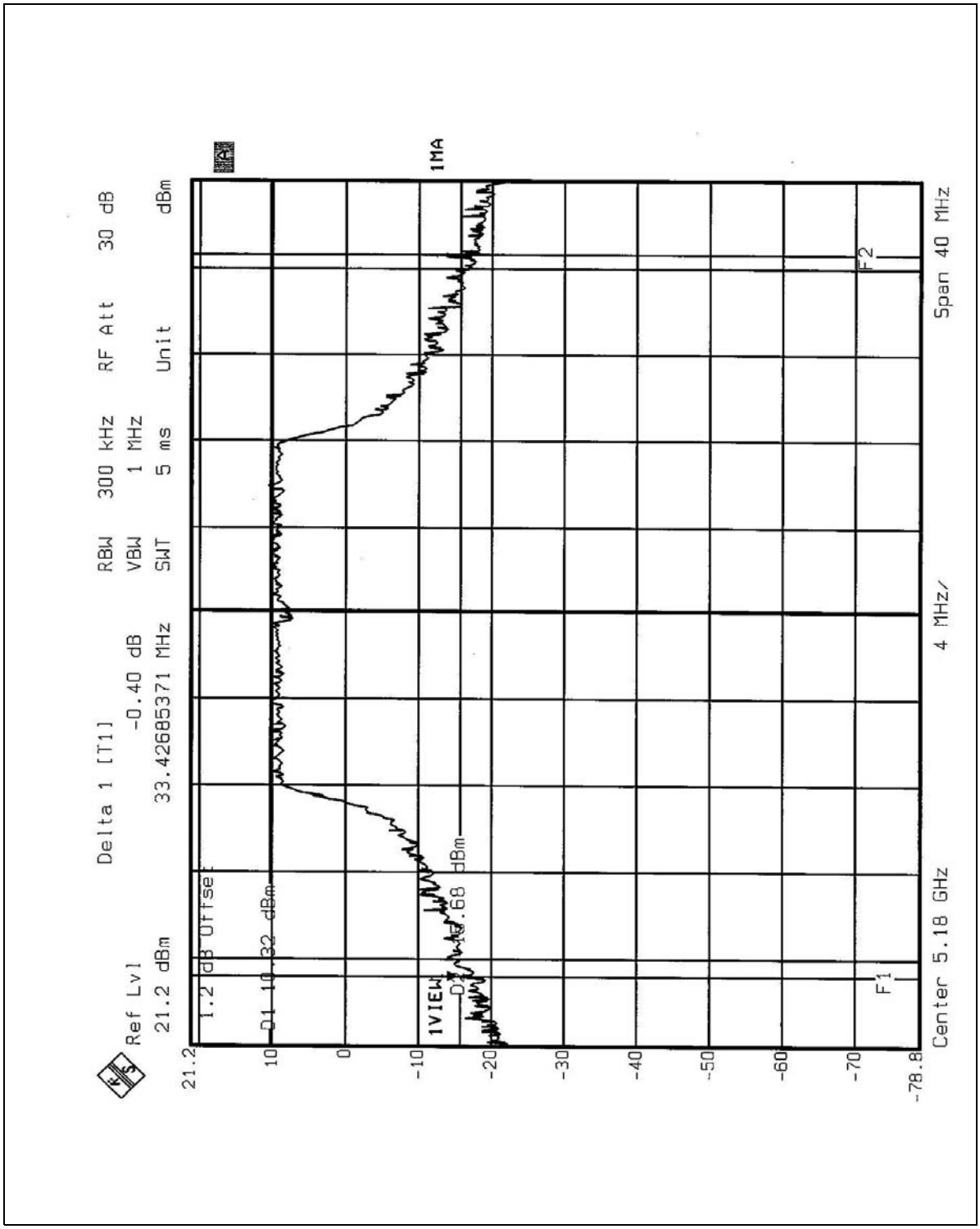
Delta 1 [T1]
-0.40 dB
33.42685371 MHz
RBW 300 kHz
VBW 1 MHz
SWT 5 ms
RF Att 30 dB
Unit dBm
Ref Lvl
21.2 dBm
1.2 dB Offset
D1 10.32 dBm
1VIEW
D2 -7.68 dBm
1MA
F2
F1
Span 40 MHz
4 MHz/
Center 5.18 GHz
21.2
10
0
-10
-20
-30
-40
-50
-60
-70
-78.8

CHANNEL 4

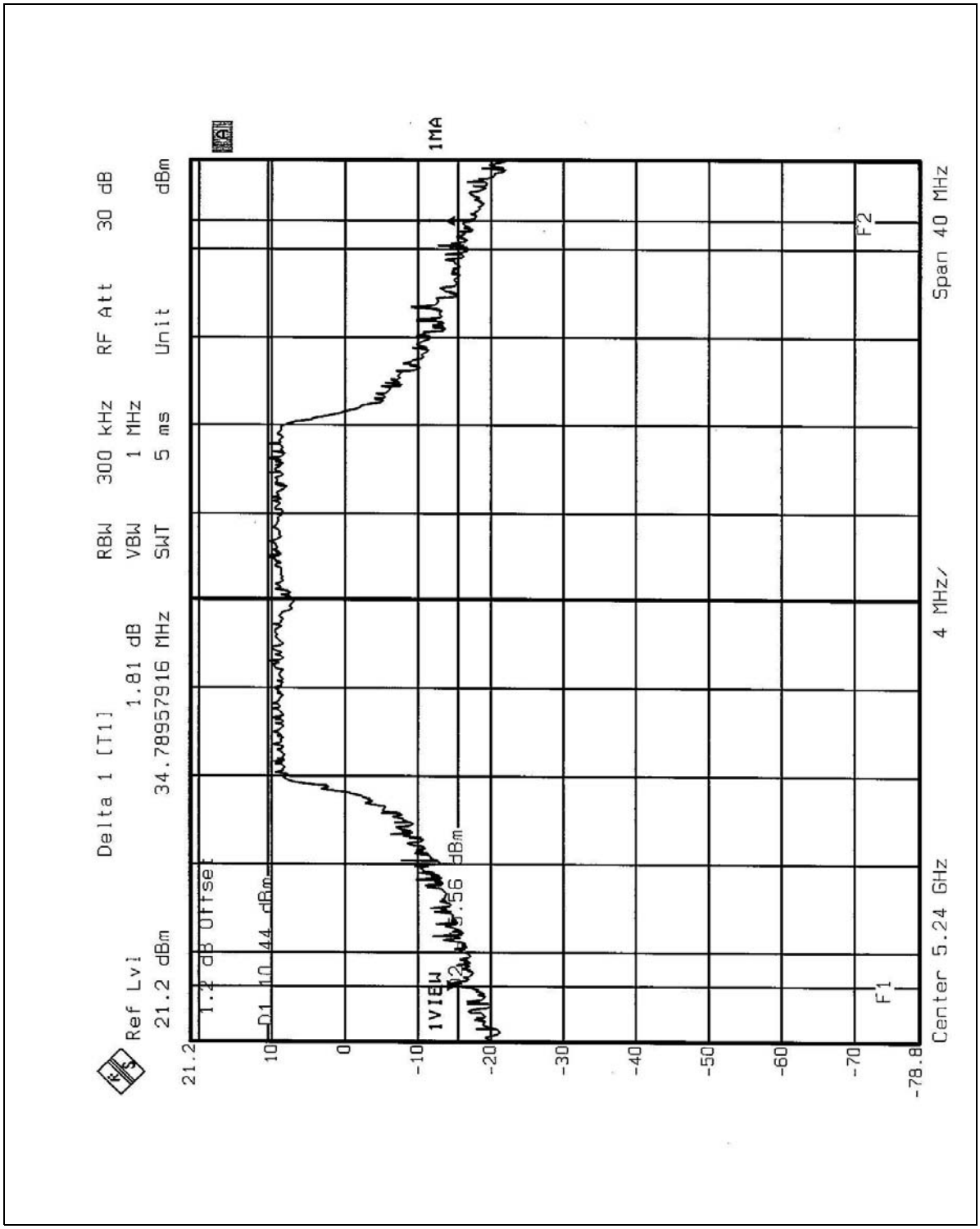
Ref Lvl
21.2 dBm
Delta 1 [T1]
1.81 dB
34.78957916 MHz
RBW 300 kHz
VBW 1 MHz
SWT 5 ms
RF Att 30 dB
Unit dBm
1MA
1VIEW
Center 5.24 GHz
4 MHz/
Span 40 MHz
F1
F2
21.2
10
0
-10
-20
-30
-40
-50
-60
-70
-78.8

CHANNEL 5

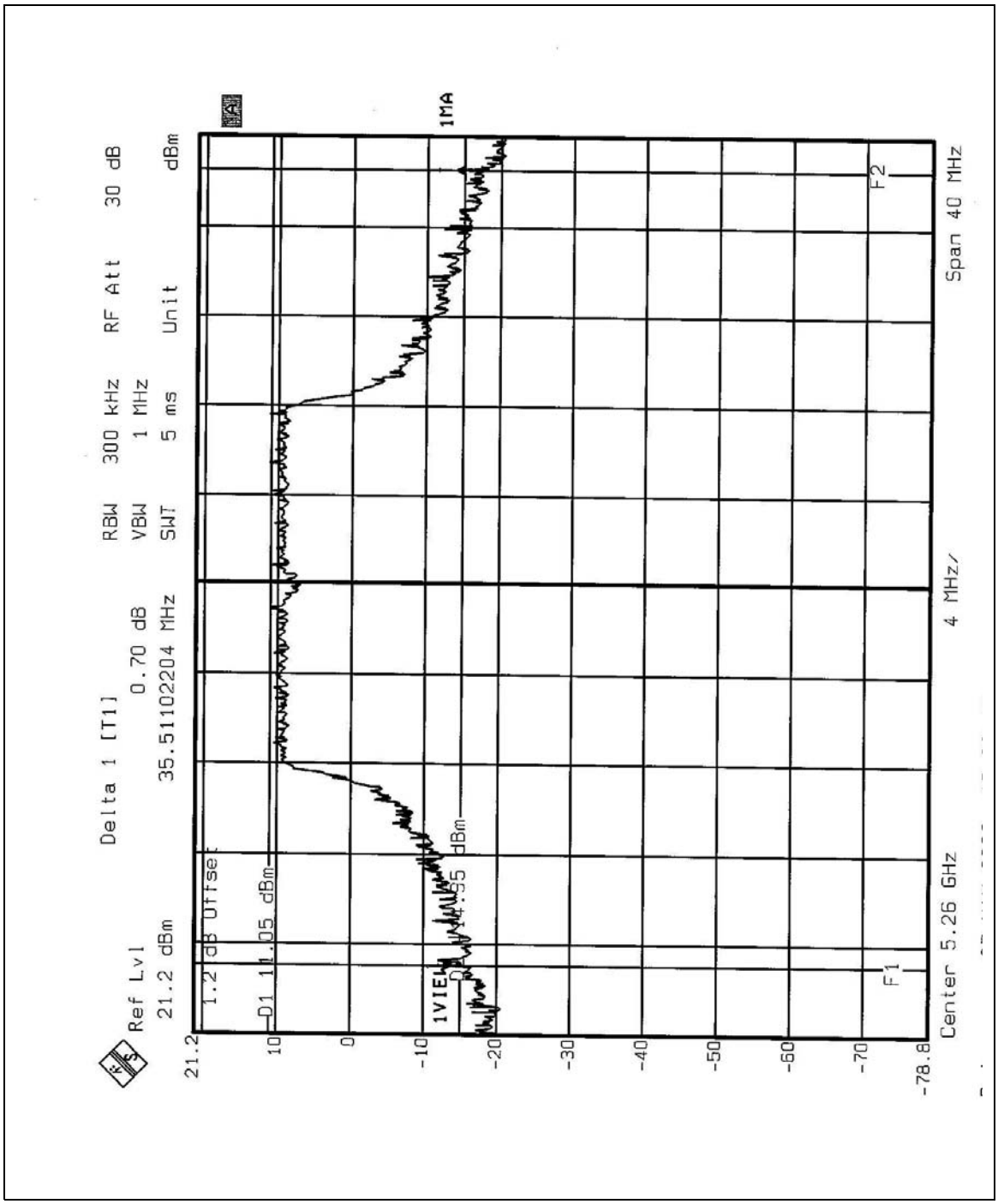
Delta 1 [T1]
0.70 dB
35.51102204 MHz
Ref Lvl
21.2 dBm
RBW 300 kHz
VBW 1 MHz
SWT 5 ms
RF Att 30 dB
Unit dBm
1MA
1VIEW
D1 11.05 dBm
1.2 dB Offset
F1
F2
Center 5.26 GHz
Span 40 MHz
4 MHz/
21.2
10
0
-10
-20
-30
-40
-50
-60
-70
-78.8

CHANNEL 8

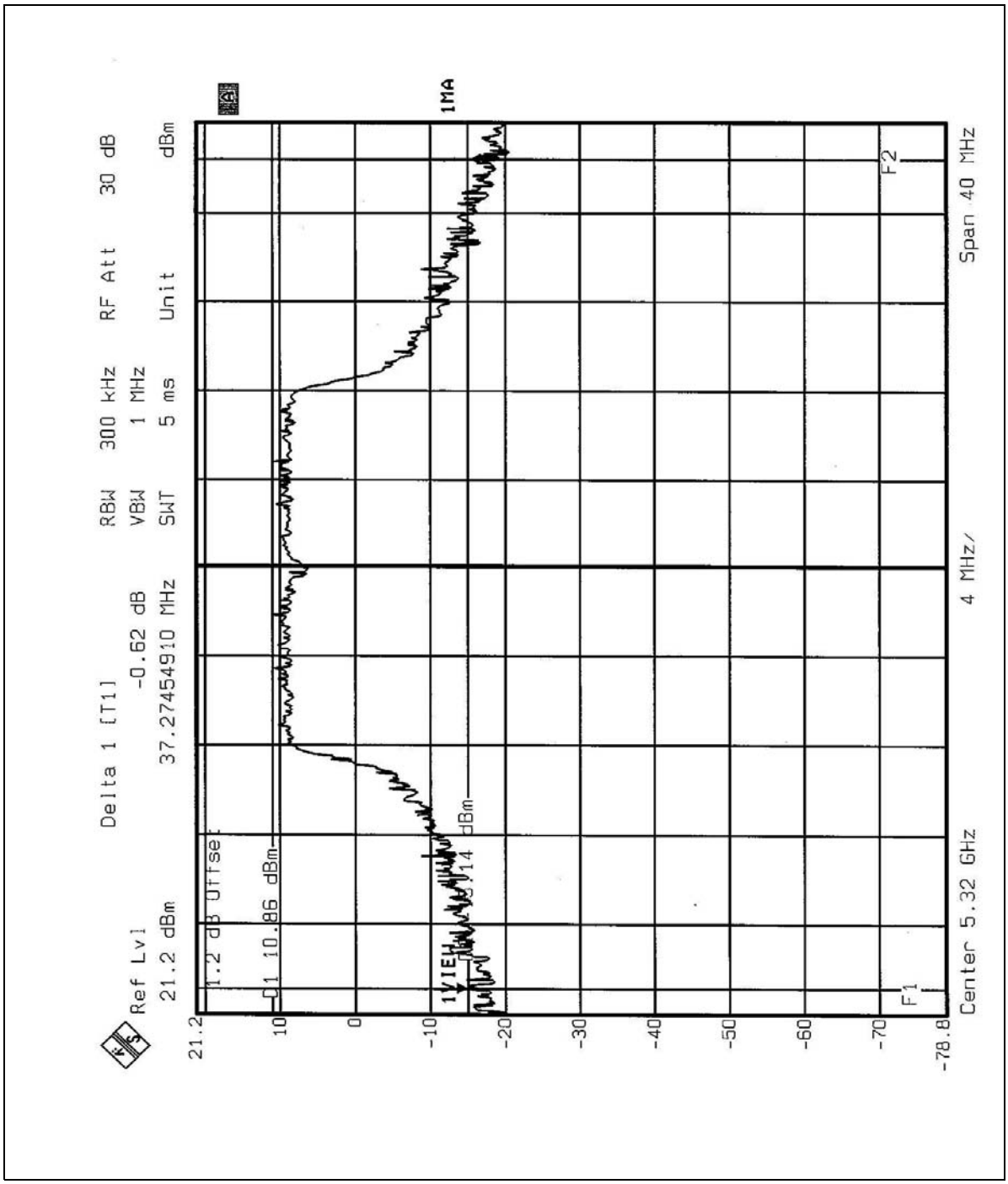
Ref Lvl
21.2 dBm
1.2 dB Offset
Delta 1 [T1]
-0.62 dB
37.27454910 MHz
RBW 300 kHz
VBW 1 MHz
SWT 5 ms
RF Att 30 dB
Unit dBm
1MA
D1 10.86 dBm
F2
F1
Center 5.32 GHz
4 MHz/
Span 40 MHz

CHANNEL9

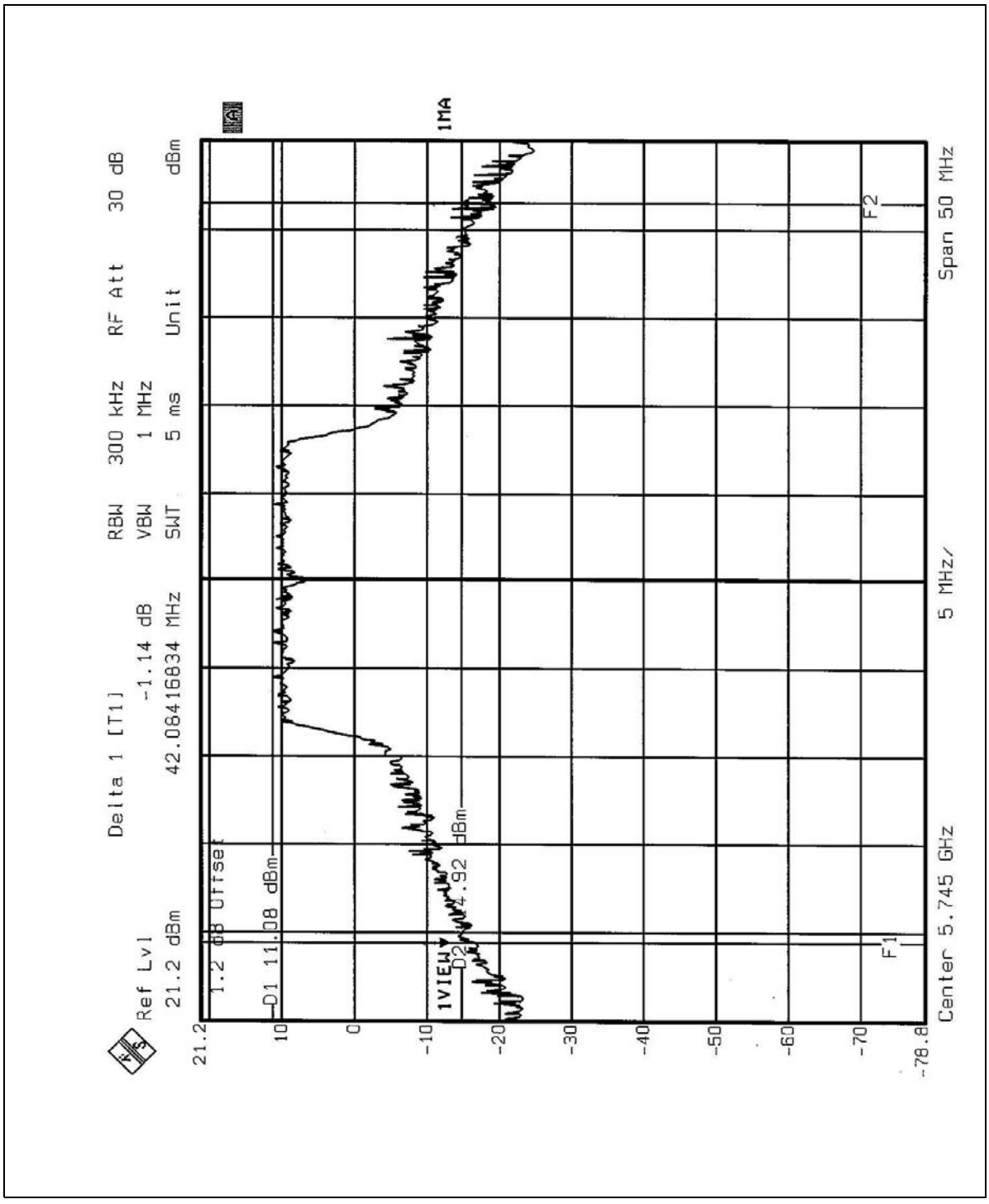
Delta 1 [T1]
-1.14 dB
42.08416834 MHz
RBW 300 kHz
VBW 1 MHz
SWT 5 ms
RF Att 30 dB
Unit dBm
Ref Lvl
21.2 dBm
1.2 dB Offset
D1 11.08 dBm
D2 -4.92 dBm
1VIEW
1MA
F1
F2
Center 5.745 GHz
5 MHz/
Span 50 MHz
21.2
10
0
-10
-20
-30
-40
-50
-60
-70
-78.8

CHANNEL12

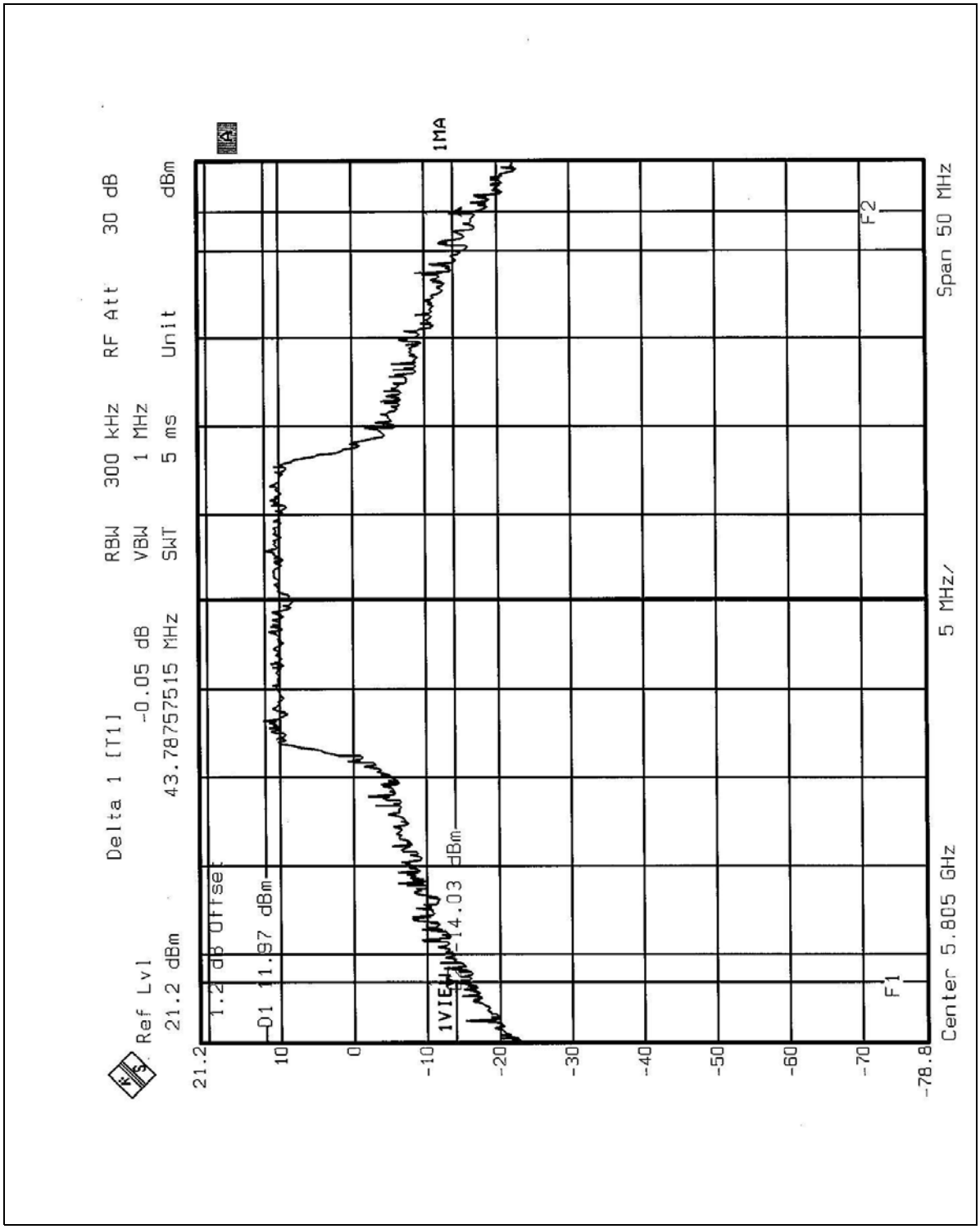
Delta 1 [T1]
-0.05 dB
43.78757515 MHz
Ref Lvl
21.2 dBm
1.2 dB Offset
D1 11.97 dBm
1VIEW -14.03 dBm
RBW 300 kHz
VBW 1 MHz
SWT 5 ms
RF Att 30 dB
Unit dBm
1MA
F2
F1
Span 50 MHz
5 MHz/
Center 5.805 GHz
21.2
10
0
-10
-20
-30
-40
-50
-60
-70
-78.8